

**EFFECTS OF FREQUENCY ON THE TEMPORAL  
SUMMATION IN THE PACINIAN PSYCHOPHYSICAL  
CHANNEL**

by

**Deniz Kılınç**

B.Sc. in Biomedical Engineering, Erciyes University, 2013

Submitted to the Institute of Biomedical Engineering

in partial fulfillment of the requirements

for the degree of

Master of Science

in

Biomedical Engineering

Boğaziçi University

2017

**EFFECTS OF FREQUENCY ON THE TEMPORAL  
SUMMATION IN THE PACINIAN PSYCHOPHYSICAL  
CHANNEL**

**APPROVED BY:**

Assoc. Prof. Dr. Burak Güçlü .....  
(Thesis Advisor)

Assist. Prof. Dr. Esin Öztürk Işık .....

Assist. Prof. Dr. Mustafa Zahid Yıldız .....

**DATE OF APPROVAL:**

## ACKNOWLEDGMENTS

I would like to express my gratitude to my advisor, Assoc. Prof. Burak Güçlü, for his invaluable guidance and support which made it possible to complete this thesis. Without his immense knowledge, great enthusiasm and endless encouragement, this work would not have been possible.

I would particularly like to thank to all participants who voluntarily spent their valuable time contributing to this study in a tight schedule.

I have had the support and encouragement of my lab mates. I thank to Assist. Prof. İsmail Devecioğlu for his technical support. I also thank to Sedef Yusufogulları, İpek Karakuş, Bige Vardar, and Agah Karakuzu whose constant motivation and sympathetic attitude during my research helped me a lot to focus on my work continuously.

I also offer my deepest gratitude to Ahmet Bülbül for his patience and unconditional support throughout this process.

Finally, I must express my most profound gratitude to my mom and dad for supporting me emotionally and spiritually throughout writing this thesis and my life in general.

## ACADEMIC ETHICS AND INTEGRITY STATEMENT

I, Deniz Kılınç, hereby certify that I am aware of the Academic Ethics and Integrity Policy issued by the Council of Higher Education (YÖK) and I fully acknowledge all the consequences due to its violation by plagiarism or any other way.

Name :

---

Signature:

---

Date:

---

## ABSTRACT

### EFFECTS OF FREQUENCY ON THE TEMPORAL SUMMATION IN THE PACINIAN PSYCHOPHYSICAL CHANNEL

According to the temporal summation theory, increasing stimulus duration causes a decrease in detection psychophysical threshold. Unlike previous psychophysical studies based on the fast adaptive tracking procedure, in this thesis, psychometric functions of the Pacinian channel were measured with the method of constant stimuli to investigate the effects of frequency on temporal summation in more detail. Six female and four male subjects (age: 25-30) participated in the experiment. Sinusoidal bursts of mechanical displacement were applied on the middle fingertip of each subject by using a cylindrical contactor ( $r = 2$  mm) at six frequencies (100, 150, 250, 350, 500, and 750 Hz), and five durations (10, 30, 100, 300, and 1000 ms). For each frequency-duration pair, six different amplitudes were used with 40 repetitions to obtain detection probabilities in a two-interval forced-choice task. The data points were fitted by sigmoidal curves to find psychometric functions. Average goodness of fits ( $R^2$ ) was 0.88. Midpoints and the slopes of psychometric curves were statistically analyzed. Following aligned rank transform, repeated measures ANOVA was used to study the effects of duration, frequency and their interaction. As expected, the thresholds had the characteristic U-shape ( $F(5,45) = 42.50, p < 0.001$ ); the slopes had an inverted U-shape ( $F(5,45) = 29.64, p < 0.001$ ). Both thresholds ( $F(4,36) = 60.34, p < 0.001$ ) and slopes ( $F(4,36) = 26.58, p < 0.001$ ) were affected by duration due to temporal summation. However, there was no interaction between frequency and duration for the thresholds ( $F(1,9) = 4.84, p = 0.055$ ), which means that temporal summation in the Pacinian channel does not significantly vary with frequency.

**Keywords:** Touch, somatosensory, psychophysics, psychometric function, temporal summation, Pacinian channel, vibrotactile stimulation.

## ÖZET

### PACİNİ PSİKOFİZİKSEL KANALINDA FREKANSIN ZAMANSAL TOPLAMAYA ETKİSİ

Zamansal toplama teorisine göre uyaran süresindeki artış algılama eşiğinde bir azalmaya sebep olmaktadır. Hızlı uyarlanırlı izleme yöntemine dayanan önceki psikofizik çalışmaların aksine, bu tezde frekansın zamansal toplamaya etkisini bulmak için Pacini kanalının psikometrik fonksiyonları sabit uyaran metoduyla ölçülmüştür. Bu çalışmada altı kadın ve dört erkekten oluşan (yaş 25-30) 10 gönüllü katılımcı yer almıştır. Katılımcıların orta el parmak uçlarına yarıçapı 2 mm olan silindirik bir prob aracılığıyla altı farklı frekans (100, 150, 250, 350, 500 ve 750 Hz) ve beş farklı sürede (10, 30, 100, 300 ve 1000 ms) sinüzoidal mekanik uyarılar verilmiştir. Her frekans-süre kombinasyonu için 40 kez tekrarlanan altı farklı genlik seviyesi kullanılarak algılama olasılıkları zorlanmış seçim göreviyle ölçülmüştür. Psikometrik fonksiyonları bulmak için deney verileri sigmoid eğrilere uydurulmuştur.  $R^2$  değerleri genelde yüksek çıkmıştır (ortalama 0.88). Psikometrik eğrilerden elde edilen orta noktalar ve eğimler istatistiksel olarak analiz edilmiştir. Hizalanmış rank dönüşümü yapıldıktan sonra, süre, frekans ve süre\*frekans ilişkisinin etkilerini incelemek için tekrarlı ölçümler ANOVA testi kullanılmıştır. Beklenildiği üzere psikofiziksel eşik değerleri karakteristik U eğrisi şeklinde bulunmuştur ( $F(5,45) = 29.64, p < 0.001$ ). Psikometrik eğimler ise ters U eğrisi şeklinde bulunmuştur. Fakat, eğimlerin ters U şeklinde olduğu görülmüştür ( $F(5,45) = 29.64, p < 0.001$ ). Hem eşik değerleri ( $F(4,36) = 60.34, p < 0.001$ ) hem de eğimler ( $F(4,36) = 26.58, p < 0.001$ ) zamansal toplama nedeniyle uyaran süresinden etkilenmiştir. Fakat eşik değerleri açısından frekans ve süre arasında bir etkileşim bulunamamıştır ( $F(1,9) = 4.84, p = 0.055$ ). Bu da Pacini kanalındaki zamansal toplamanın frekansa göre istatistiksel anlamlı olarak değişmediğini göstermektedir.

**Anahtar Sözcükler:** Dokunma, beden duyusu, psikofizik, psikometrik fonksiyon, zamansal toplama, Pacini kanalı, mekanik-titreşimsel uyarm.

## TABLE OF CONTENTS

ACKNOWLEDGMENTS . . . . .	iii
ACADEMIC ETHICS AND INTEGRITY STATEMENT . . . . .	iv
ABSTRACT . . . . .	v
ÖZET . . . . .	vi
LIST OF FIGURES . . . . .	ix
LIST OF TABLES . . . . .	xi
LIST OF SYMBOLS . . . . .	xii
LIST OF ABBREVIATIONS . . . . .	xiii
1. INTRODUCTION . . . . .	1
1.1 Motivation . . . . .	1
1.2 Hypothesis . . . . .	1
1.3 Outline . . . . .	2
2. THEORY . . . . .	3
2.1 Skin Anatomy . . . . .	3
2.2 Mechanoreceptors in Glabrous Skin . . . . .	4
2.3 Mechanoelectric Transduction . . . . .	7
2.4 Sensory Pathway . . . . .	7
2.5 Psychophysics and Psychophysical Methods for Measurement of Sensation	10
2.6 Physiological Properties of Mechanoreceptors . . . . .	11
2.7 Four Channel Model in Tactile Psychophysics . . . . .	13
2.8 Temporal Summation . . . . .	16
3. METHODOLOGY . . . . .	24
3.1 Subjects . . . . .	24
3.2 Apparatus . . . . .	24
3.3 Stimuli . . . . .	26
3.4 Procedure . . . . .	27
3.5 Data Analysis . . . . .	28
4. RESULTS . . . . .	29
4.1 Psychometric Functions . . . . .	29

4.2 Effects of Frequency on Temporal Summation . . . . . 37

4.3 Threshold Shift . . . . . 39

5. DISCUSSION . . . . . 41

5.1 Effects of Frequency on Threshold and Slope of Psychometric Function 41

5.2 Temporal Summation in Pacinian Channel . . . . . 42

5.3 Effects of Frequency on Temporal Summation . . . . . 44

5.4 Limitations . . . . . 45

5.5 Future Work . . . . . 46

REFERENCES . . . . . 47





## LIST OF FIGURES

Figure 2.1	Layers of the skin	4
Figure 2.2	Mechanoreceptors involved in tactile sensation	5
Figure 2.3	Structures and histology of Pacinian corpuscle	6
Figure 2.4	Two-pathway transmission of somatosensory information	8
Figure 2.5	Functionally specialized columns in somatosensory cortex	9
Figure 2.6	Physiological properties of mechanoreceptive fibers	12
Figure 2.7	Four channel model of tactile perception	15
Figure 2.8	The average results of Verrillo (1965) replotted	17
Figure 2.9	Threshold shifts from previous psychophysical studies	17
Figure 2.10	The effect of stimulus duration on thresholds of P and NP channels	18
Figure 2.11	Threshold shift and burst duration curve for four response criteria	19
Figure 2.12	Threshold shift curves of theoretical model and temporal integrator	20
Figure 2.13	Frequency-response curves of the human PC fibers, human P-channel and cat mesentery PC fibers	21
Figure 2.14	The frequency response curves obtained with constant duration and constant cycles	22
Figure 2.15	Threshold shift graph obtained from thenar eminence and fingertip	23
Figure 3.1	Block diagram of the experimental setup.	25
Figure 3.2	Experimental setup and isolated room	25
Figure 3.3	Shaker and hand position of the experiment	26
Figure 3.4	Timing diagram of experiment.	27
Figure 4.1	Psychometric curves of subject-2 at 100 Hz for all durations	31
Figure 4.2	Psychometric curves of subject-2 at 150 Hz for all durations	32
Figure 4.3	Psychometric curves of subject-2 at 250 Hz for all durations	33
Figure 4.4	Psychometric curves of subject-2 at 350 Hz for all durations	34
Figure 4.5	Psychometric curves of subject-2 at 500 Hz for all durations	35
Figure 4.6	Psychometric curves of subject-2 at 750 Hz for all durations	36
Figure 4.7	Frequency-threshold curves of 10 subjects for all durations.	38

Figure 4.8	The relationship between displacement threshold ( $\alpha$ ) and frequency for all durations	39
Figure 4.9	The relationship between psychometric slope ( $1/8\beta$ ) and frequency for all durations	39
Figure 4.10	The relationship of average threshold shift relative to 1000 ms and duration	40
Figure 5.1	Temporal summation for two different contactor sizes in the constant population model	43



## LIST OF TABLES

Table 4.1	Averages of threshold and slope values which were obtained from psychometric function for 100 Hz.	29
Table 4.2	Averages of threshold and slope values which were obtained from psychometric function for 150, 250, 350, 500 and 750 Hz.	30
Table 4.3	Threshold decrease per doubling of stimulus duration between 10 ms and 100 ms for each frequency	40



## LIST OF SYMBOLS

$p$	Probability
$t, d$	Stimulus duration
$v, f$	Frequency
$T$	Period
$n$	Number of cycles
$\alpha$	Midpoint of the sigmoid curve
$\beta$	The parameter related to the slope of the sigmoid curve
$p_c$	Probability of correct detection
$A$	Amplitude
$R^2$	Goodness of fit
$Na^+$	Sodium ion
$K^+$	Potassium ion
$Hz$	Hertz
$s$	Seconds
$dB$	Decibel

## LIST OF ABBREVIATIONS

RA	Rapidly adapting
SA	Slowly adapting
PC	Pacinian afferent
SAI	Slowly adapting type I afferent
SAII	Slowly adapting type II afferent
DCN	Dorsal column nuclei
CNS	Central nervous system
SI	Primary somatosensory cortex
SII	Secondary somatosensory cortex
P	Pacinian channel
NP	Non-Pacinian channel
LED	Light emitting diode
dB re $1\mu\text{m}$	Decibel referenced to $1\mu\text{m}$
Th	Threshold
TS	Threshold shift

# 1. INTRODUCTION

## 1.1 Motivation

Tactile perception is one of the most important sensation to gather information about the surroundings and to conduct daily activities. There is an increasing number of people who suffer from injuries, neural disorders and illnesses that cause losing their tactile sensations and motion abilities. Over the past decade, these patients have controlled neural prostheses by their own neural activity which gives effective movement capability [1]. However, without sensory feedback, patients cannot either adjust the forces applied on objects or discriminate the features of the objects [2]. In order to create reproducible perception, electrical stimulation should be applied on peripheral nerve or somatosensory cortex [3]. In order to develop these prostheses, somatosensory mechanisms should be investigated. One of the important components of somatosensation is temporal summation, in which psychophysical detection thresholds decrease as the stimulus duration increases [4]. When designing the algorithms of neuroprostheses, it should be considered that how brain processes the longer vibrotactile stimuli and how the sensors of the neuroprostheses should process them. That is why, understanding the mechanisms of temporal summation of mechanoreceptors is helpful.

## 1.2 Hypothesis

The aim of this thesis was to investigate the temporal summation in the Pacinian psychophysical channel. In the literature, temporal summation was studied based on the fast adaptive tracking procedure specifically at thenar eminence with a limited range of frequency and duration combinations. However, the detailed information about the effect of frequency on temporal summation does not exist. Additionally, most of the previous work was not done on the fingertip which has largest innervation density of the mechanoreceptors. Therefore, the main novelty of this work was to look

at frequency effects in the Pacinian channel with the method of constant stimuli in which psychometric curves were obtained.

The classical neural integration model predicts a decrease in threshold as the vibrotactile frequency increases at a given duration. However, the difference of thresholds obtained at two durations is expected to stay constant as the frequency is increased. As a matter of fact, our previous work showed that the temporal summation was not much affected by frequency [5]. That experiment was performed by an adaptive tracking procedure which converges to a single point on the psychometric function. I obtained the full psychometric function by the method of constant stimuli, and studied both threshold and slope obtained from this function. I hypothesized that there should be a threshold shift in the psychophysical Pacinian channel, which would not be affected at different frequencies, as the stimulus duration increases.

### **1.3 Outline**

In the first chapter, motivation and hypothesis of the study were presented. In the second chapter, skin anatomy, anatomy and physiology of mechanoreceptors, sensory pathway, four channel model and temporal summation in the Pacinian channel were explained. In chapter 3, methodology of this study were explained. The results of the experiments were presented in the chapter 4. In the last chapter, the general conclusion and future work of the study were discussed.

## 2. THEORY

### 2.1 Skin Anatomy

Skin is the largest organ of the body which consists of mechanoreceptors, nerve fibers, sweat glands, blood vessels and other structures. It is divided into three types: glabrous skin that is observed generally on the skin of palm and sole, hairy skin and mucocutaneous skin, which exist on the interior surface of the body. These three types have different substructures which give them specific mechanical characteristics, so they have different sensory capabilities [6].

Glabrous and hairy skin have three layers, which are namely *epidermis* (outer layer), *dermis* (inner layer) and *hypodermis* (subcutaneous tissue). Figure 2.1 shows the layers of the skin. Also, the outer layer is covered by the *stratum corneum* which consists of dead cells and creates a tough surface. Thickness of the stratum corneum is approximately 10-25  $\mu\text{m}$  [7]. There is a border between epidermis and dermis called *dermal-epidermal junction* that contains specialized epithelial (somatic) cells. These cells start to die when they migrate towards the outer parts of the skin and become a part of the stratum corneum. Another role of this junction is providing a physical barrier that impedes the crossing of large molecules and cells [8].

The epidermis, which is 30-100  $\mu\text{m}$  thick, is composed of epithelial cells. Because of less intracellular space, epidermis has a stronger mechanical integrity than other soft tissues [9]. Also, it does not have blood supply; so the nutrients epidermis needs come to plasma from the dermis through epidermal-dermal junction. However, the dermis contains blood vessels, fat cells, sweat glands, lymphatic vessels, mechanoreceptors and nerve fibers.

The dermis has 1-4 mm thickness and constitutes 15-20% of the total body weight [10]. Moreover, it is made of connective tissue and elastic fibers which provide a semi-fluid constitution [11]. After deformation, elastic fibers ensure the recovery of the skin shape. Furthermore, semi-fluid constitution impedes the leakage of the dermis, even under high pressures [8].



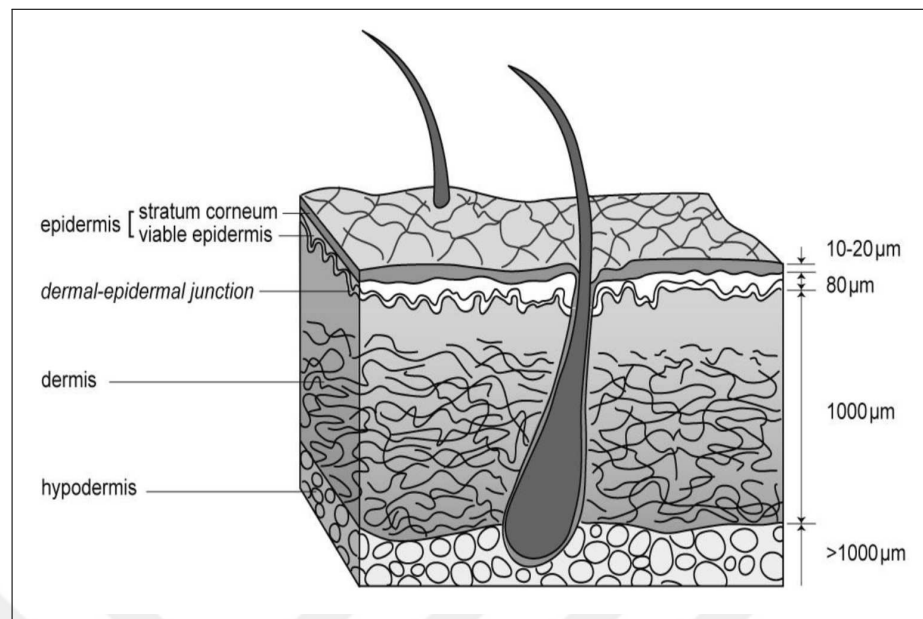


**Figure 2.1** Layers of the skin [8].

The third layer is the hypodermis (subcutaneous fat) which has a varied thickness that changes depending on the age, sex and anatomical regions of the individual. It is formed by a loose fatty connective tissue. The role of the hypodermis is protecting the skin against external pressures [10].

According to the physical standpoint, the skin has diverse mechanical properties due to its incompressible viscoelastic structure. When a mechanical stimulus is applied on the skin, stress and strains are produced in the skin. In the previous studies, it is stated that deformation or strain is an adequate stimulus in order to initiate transduction in tactile receptors. Yet, stress is less relevant to tactile sensation [12].

## 2.2 Mechanoreceptors in Glabrous Skin

When an individual touches an object, a deformation in the form of displacement and indentation occurs in the skin. This deformation stretches the tissue; therefore, it stimulates the sensory endings of mechanoreceptors under contact region [13]. According to anatomical and electrophysiological experiments, there are four types

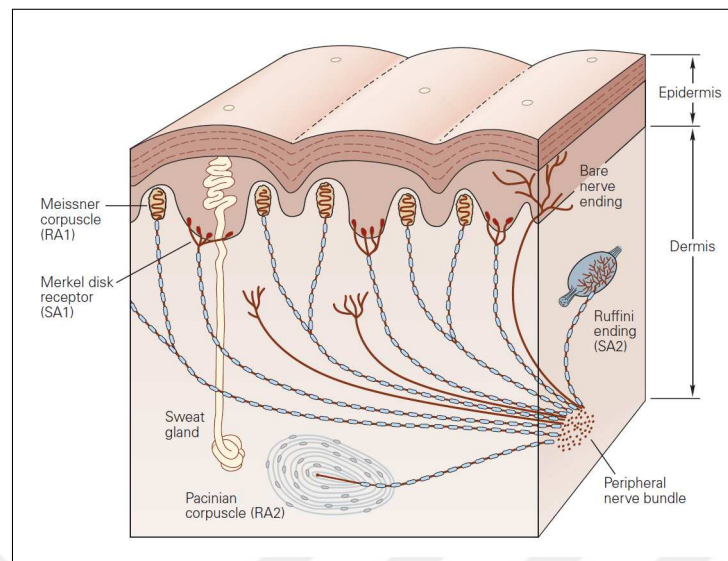


**Figure 2.2** Mechanoreceptors which are involved in tactile sensation [13].

of mechanoreceptors in the glabrous skin that are referred to as Pacinian corpuscles, Meissner's corpuscles, Merkel's discs and Ruffini endings [14]. These mechanoreceptors are innervated by nerve fibers that are *PC*, *RA*, *SAI* and *SAII*, respectively. Each of the receptors has a different response characteristic to tactile stimulation due to their structures [15]. Figure 2.2 demonstrates that some of the mechanoreceptors have a non-neural structure which are called accessory structures. It is thought that accessory structures have a role in filtering mechanism [16].

As SAI fibers reach the epidermis, they branch out over a large area, lose their myelin and innervate a large number of Merkel cells [17]. The unmyelinated ends of SAI fibers are enfolded by specialized epidermal cells (Merkel) in the basal layer of the epidermis [18].

RA afferent fibers innervate the disk-like endings within Meissner's corpuscles. The unmyelinated part of them reside between the sweat ducts and adhesive ridges, so RA fibers are closer to surface of the epidermis than other mechanoreceptors within the dermis [19]. Therefore, it is thought that RA fibers are more sensitive to minimal skin deformation than SAI fibers.

The large encapsulated endings of Pacinian corpuscles located in the deeper part of the dermis are innervated by PC fibers without branching. It has an onion-like capsule shown in 2.3(a) and 2.3(b), which contains a series of lamellae of connective

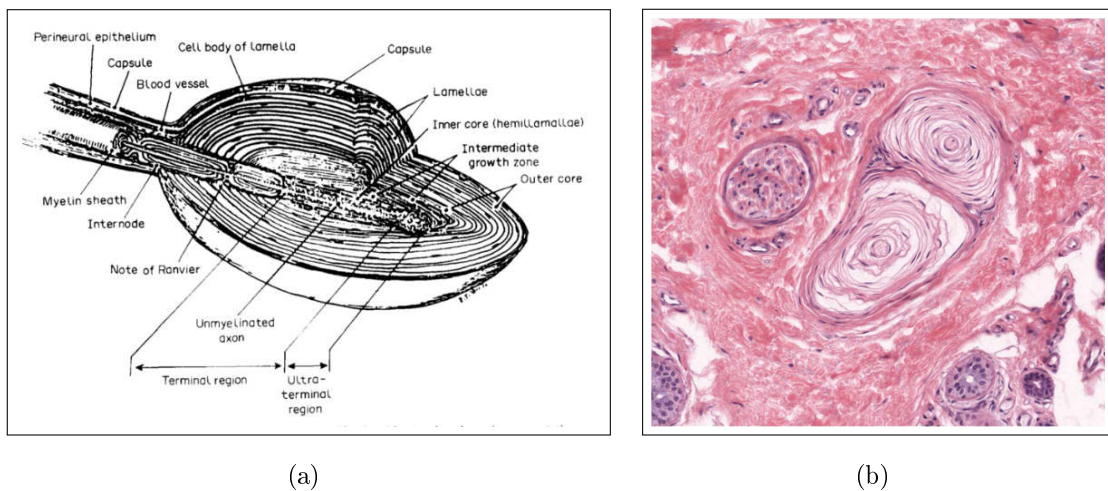


**Figure 2.3** (a) Structures of Pacinian Corpuscles [20]. (b) The slice of the skin which shows two neighboring Pacinian Corpuscles [21]

tissue separated by a fluid-filled space [22]. The capsule is composed of outer core, intermediate growth zone, inner core and neurite. The single unmyelinated PC ending (neurite) and its myelinated axon that extends to Ranvier node are surrounded by an inner core which includes Schwann cells [23, 24]. The intermediate growth zone which is visible in immature Pacinian corpuscles resides between the inner core and the outer core. The cells of mature ones become incorporated into the inner core or the outer core. The outer part is made of 30 concentrically arranged lamellae that include flat epithelial cells and collagenous fibrils [23]. Each lamella is separated by fluid-filled space which contributes to filtering of vibrotactile stimuli between the outer core and neurite [11]. Also, there is a capsule which encloses outer core. The capsule behaves as a high-pass filter, which only transmits disturbances at high frequencies to stimulate the nerve endings. Also, it amplifies the high-frequency stimuli. If dynamic strains and stresses were not filtered by the fluid-filled corpuscle, the sensitive Pacinian corpuscles would be overwhelmed by the excessive stimulation [15].

Ruffini endings which are innervated by SAIL afferent fibers are densely located at the finger, wrist joints and skin folds in the palm. They are enclosed by spindle-shaped capsules that contain collagen fibrils. The long axis of the corpuscle resides parallel to stretch line; so they respond to cutaneous stretching. Because of the large size of Ruffini endings and Pacinian corpuscles, they can sense the stimuli that are far from the sensory endings [13].

## 2.3 Mechanoelectric Transduction

When the skin is deformed by a mechanical stimulus, accessory structures behave like a mechanical filter and conduct the strain to the unmyelinated membrane [25]. After stretch sensitive channels are activated by the strain, conductance of the channels to certain cations ( $\text{Na}^+$  and  $\text{K}^+$ ) increases, which causes the receptor potential at short latency [26]. If there is sufficiently high receptor potential, an action potential will be produced in the first node of Ranvier and transmitted along peripheral axon [17]. This mechanism transduces the mechanical energy to electrical energy.

It is important that receptor potential and action potential are generated at different sites [27, 28]. The unmyelinated part of the neurite is responsible for receptor potential; whereas the action potential arises in the first node of Ranvier [29, 30]. Specifically, it is thought that filopodias, which extend from the unmyelinated neurite have a role in receptor potential [31].

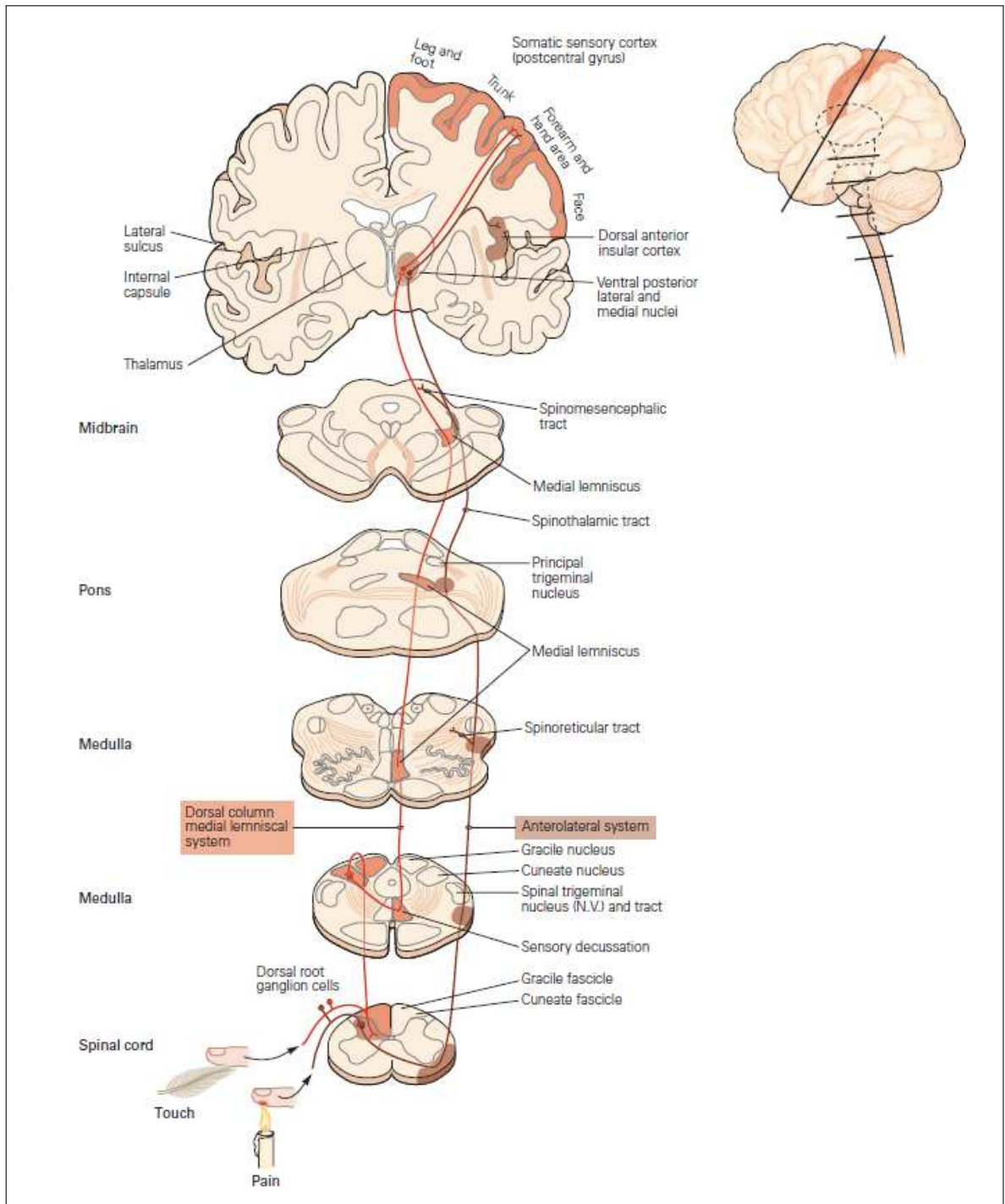
When the effect of stimulus amplitude is considered, there is a linear relationship between receptor potential and stimulus amplitude at low stimulus amplitudes. However, a saturation occurs at high amplitude stimuli [32]. As the magnitude of receptor potential increases, the firing rate of action potential increases.

## 2.4 Sensory Pathway

Due to mechanical stimulation of the mechanoreceptors, a mechanoelectric transduction generating neural activity occurs in the skin. While the unmyelinated nerve terminal is capable of mechanoelectric transduction, the myelinated nerve fibers transmit the action potential. There is no synapse between the site of mechanoelectric transduction and of action potential production; therefore, tactile mechanoreceptors are known

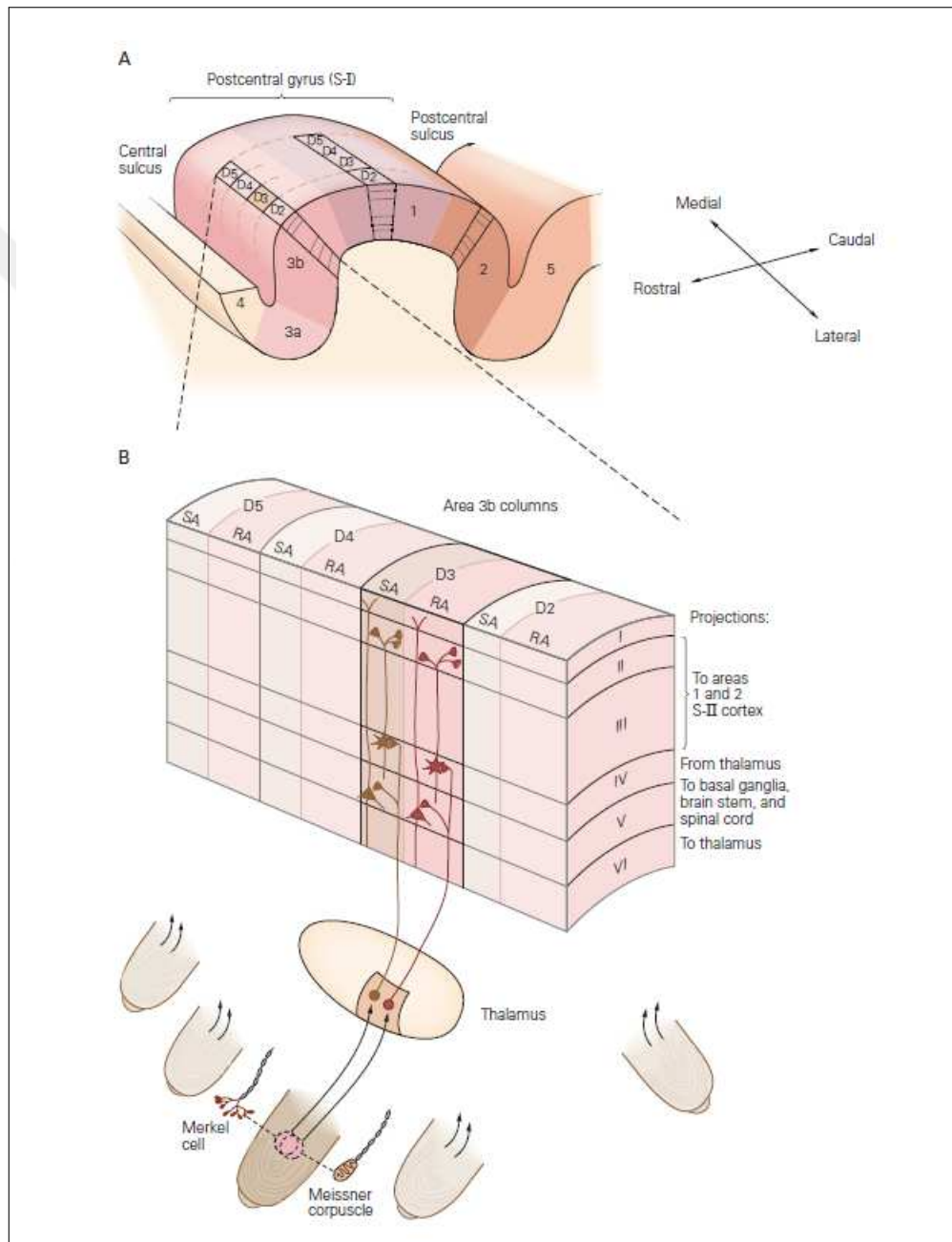
as *primary receptors* [33].

Figure 2.4 illustrates that this information is carried to *dorsal root ganglia* that consists of cell bodies of mechanoreceptive neurons and enter the dorsal aspect



**Figure 2.4** Somatosensory information is transmitted from mechanoreceptors to CNS by two pathway [13].

of the spinal cord. Then, it is transmitted by the *dorsal column* to *dorsal column nuclei (DCN)* which resides in the brain stem. After the first synapse is made in DCN, the neurons, referred to as *second-order neurons of somatosensation*, make the second synapse in the thalamus. This pathway is called *medial lemniscal system*. The sensory information is processed in the thalamus and the output is conveyed to the *primary*



**Figure 2.5** Functionally specialized columns in somatosensory cortex [13]. (A) A columnar organization of somatosensory cortex. (B) A portion of area 3b which receives inputs from adjacent fingers.

*somatosensory cortex (SI)* and *secondary somatosensory cortex (SII)* that are located in the parietal lobe [25].

In the somatosensory cortex, there are specialized columns as an anatomical structure which contains neurons. These neurons have inputs from a certain area of receptor sheets in the body and responds to the same receptors. Only one submodality, such as pressure or vibration, is processed by these neurons. Neighboring columns receive information from neighboring fingers through SA and RA fibers, which are shown in figure 2.5 [13].

## 2.5 Psychophysics and Psychophysical Methods for Measurement of Sensation

Psychophysics examines the relationship between physical stimuli and sensation. The main concept of the psychophysics is sensory threshold. Weber and Fechner studied the sensitivity of sensory organs and introduced experimental and mathematical techniques to measure the weakest detectable sensation. They defined the *absolute threshold* as the lowest strength of the stimulus detected by a subject. Also, the difference in stimulus intensity that is just noticeable was termed *difference threshold*. In 1883, Weber developed a paradigm to understand how a subject discriminates two stimuli with different amplitudes. According to Weber's law, the amount of the difference threshold was linearly related with stimulus intensity [34]. Although Fechner (1860) claimed that there was a logarithmic relationship between stimulus strength and intensity of sensation, Stevens (1953) showed that this relationship was best explained with a power function [13].

Fechner's methods for measuring the sensory performance made important contributions to psychophysics. There are three general methods originally developed by Fechner that are still used in psychophysical experiments. First, the method of constant stimuli in which a constant set of stimuli is repeatedly presented to subject. For example, in absolute threshold measurement, as the intensity of stimulus increases,

the probability of detection of the stimulus also increases. The second method is the method of limits, which is less time consuming but also less precise than the method of constant stimuli. In this method, stimulus intensity changes continuously in ascending or descending order. The intensity level when the subject detects the stimulus in ascending order or stops detecting the stimulus in descending order is recorded. In order to find absolute threshold, these two points are averaged. The third is the method of adjustment which is mostly used to measure difference thresholds. A stimulus at a certain intensity is presented to subject. Then, the subject adjust stimulus intensity until it equals to first stimulus [13, 34].

In modern psychophysics two-alternative forced-choice (2AFC) tasks are used to eliminate subject's criterion. For example, in the two-interval forced-choice task the subjects choose one of the two interval for the test stimulus. Forced-choice task can be used with adaptive tracking methods and the method of constant stimuli. In this thesis, the points on the psychometric functions were found by using the method of constant stimuli in a two-interval forced-choice task. [34].

## 2.6 Physiological Properties of Mechanoreceptors

When the psychophysical and neurophysiological studies are considered, each afferent nerve fiber that mediates mechanoreceptors has a distinct perceptual function. Mechanoreceptors are classified in accordance with their adaptation type and receptor field size. Pacinian corpuscles, Meissner's corpuscles, Merkel's discs and Ruffini endings are mediated by nerve fibers that are PC (FAII), RA (FAI), SAI and SAII, respectively [33, 35, 36, 37]. When a stimulus is applied on the skin for several seconds at the same position and amplitude, the neural activity decreases and sensation disappears. This is called *receptor adaptation* [13]. There are two types of adaptation in afferent fibers that are FA (fast adaptation) and SA (slow adaptation) which are divided into subgroups: FAI, FAII, SAI, SAII. Figure 2.6 shows that FAI mechanoreceptors create a response during the ramp portion of the vibration whereas FAIIs give response to only corners of the waveform. On the other hand, SAI mechanoreceptors respond to both ramp



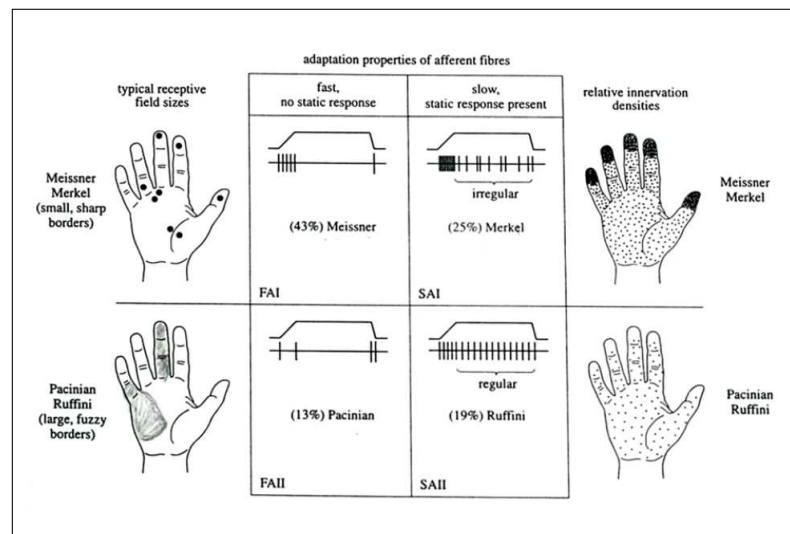


**Figure 2.6** Physiological properties of mechanoreceptive fibers in the human hand [25].

and hold part of the stimulus and show an irregular firing pattern while SAIIs have a regular firing pattern [25].

According to receptive field sizes, SAIIs and FAIIs have larger receptive fields than SAIs and FAIs. Also fingertips have a denser mechanoreceptor distribution than palms in type I afferents (FAI and SAI) [13].

SAI afferent fibers have two important properties which affect their response characteristics. First, they can discriminate points, edges and curvatures, because they are selectively sensitive to strain energy density. Second, although spatial details are smaller than their receptive field diameters (2-3 mm), they have high spatial resolution (0.5 mm). Due to these two features, a spatial neural image of a tactile stimulus is accurately conveyed by SAI afferents [15]. They have at least ten times more delicate response to dynamic stimuli than static stimuli [18].

RA fibers perceives dynamic skin deformation four times more delicately than SAI afferents due to their close location to the surface of the epidermis. Also, static skin deformation and very low frequency vibrotactile stimuli are not sensed by them probably as a result of the fluid-filled capsule which encloses the Meissner's nerve ending. Unlike the SAI fibers, they resolve spatial details which are identical to their receptive field diameter; therefore, they have a poor spatial resolution [15]. Furthermore, they are the most sensitive fibers to detect slip between an object and the skin, so the most important function of RA afferents is providing a feedback of grip control [38, 39].

PC afferent fibers have three significant response characteristics. First, they are the most sensitive fibers to respond to 10 nm of skin displacement near 200 Hz [40]. Due to their extreme sensitivity and the deep position of Pacinian corpuscles, PC fibers nearly do not have capability of spatial resolution. Second, they intensely filter the low frequency stimuli with fluid-filled lamellae in order to impede overwhelming of Pacinian corpuscles. The last one is response to a phase-locked stimuli and Poisson discharge at low frequency (less than 100-150 Hz) [41]. Poisson discharge states that a complex stimulus waveform at 30-150 Hz cannot be represented by single afferent. On the other hand, whole afferents randomly fire at a rate related to amplitude of an instantaneous stimulus, so the stimulus waveform is correctly represented [15]. Due to these response characteristics, PC fibers perceive distant events through vibrotactile stimuli during the grasping of an object [42]. Furthermore, when the object vibrating parallel to the skin surface is held, threshold is lower compared to the object which vibrates perpendicular to skin surface [41].

Among the four afferent fibers, SAI is the least effective at perception of skin indentation while it is the most sensitive to skin stretch. When it conveys information of skin stretch to central nervous system, there is only a small amount of interference which stems from the objects in the hand [18, 43]. According to the psychological and neurophysiological studies, there are two important functions of SAI afferents. First, if a skin stretch occurs during an object motion or force, SAI fibers have the ability to sense the direction of object motion or force [44]. On the other hand, perception of motion is mostly performed by RA afferents [45]. Second, they perceive the hand shape and finger position together with muscle spindles and joint fibers according to skin stretch generated by each finger and hand form [18, 46, 47].

## 2.7 Four Channel Model in Tactile Psychophysics

For investigating sensory systems, the concept of psychophysical channels has an important role. These channels are tuned to a certain area of energy spectrum a system responds. Each channel has a specific activity level which determines the prop-

erties of stimuli [48]. It is thought that the channel with the lowest threshold represent the psychophysical threshold at certain frequency. In the earliest studies, it was found that detection thresholds has U-shape at high frequencies, whereas it does not change with frequency at low frequencies [26, 49, 50]. Verrillo (1963) stated that the U-shape portion corresponds to P channel, while flat portion represents the NP channel. In order to make detailed investigation, two procedures in which one channel could be selectively isolated, selective adaptation and masking, were used.

In selective adaptation, since threshold of one channel is elevated, detection threshold of other channels could be obtained for a wide range of frequencies. With selective adaptation, NP channels were separated into two that are NPI and NP II [51]. On the other hand, if a channel's threshold is higher than another channel's threshold at a given frequency, the channel with the lower threshold can be masked by applying a high level stimulus before the test stimulus. This allows measuring thresholds of less sensitive psychophysical channels. A high level masking stimulus is presented before the test stimulus to decrease detection of test stimulus. Thus, frequency curve of the masked channel shifts upward and characteristic of other channels can be determined [52]. With the masking procedure, the existence of NPI and NP II channels was again proved [53], also NP III channel was discovered [54].

According to the study of Bolanowski (1988), there are four types of different channels which are associated with specific fibers in the glabrous skin [54]. Characteristics of the channels are obtained by altering the stimulus properties, frequency, contactor size, masking techniques and surface temperature [26, 51, 42, 55]. With respect to figure 2.7;

- Pacinian (P) channel is mediated by Pacinian corpuscles which are mostly sensitive to vibration stimulus in the range of 40-500Hz. It has a characteristic U-shape which has the most sensitive part near the range of 250-300 Hz in the threshold-frequency curve [57]. This channel is highly affected by skin-surface temperature changes [42]. Also, Pacinian channels have the ability of spatial summation which means that detection threshold decreases as the contactor size rises. However, non-Pacinian channels cannot spatially summate the stim-

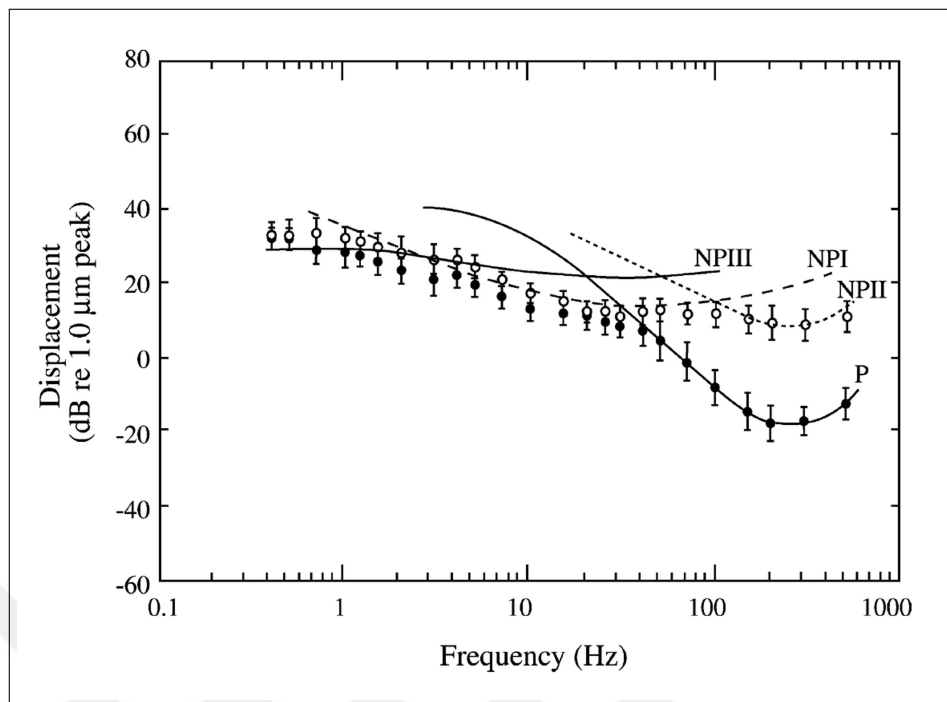


**Figure 2.7** Four channel model of tactile perception [56].

ulus. Additionally, when stimulus duration is increased, Pacinian channels have a capability of temporal summation which cause decrease in detection threshold.

- Non-Pacini I (NPI) channels are innervated by Meissner corpuscles that sense the flutter stimulation in the range of 2-40 Hz. P channel has a higher sensitivity to vibration than NPI. It is not sensitive to temperature changes [58] and not capable of temporal and spatial summation [42, 59].
- Non-Pacini II (NPII) channels are mediated by Ruffini endings which are stretch sensitive in the range of 100-500Hz. The frequency- response curve of NPII is only determined when the small contactor is used. It also cannot summate the temporal and spatial stimuli [60].
- Non-Pacini III (NPIII) channels are mediated by Merkel's cell that have sensitivity for pressure in the range of 0.4-2 Hz. The characteristics of it can be determined by either a small or a large contactor. Unlike the Pacinian channels, spatial and temporal summation is not observed in NPIII channels.

## 2.8 Temporal Summation

The temporal summation is defined as the decrease in the detection threshold with increasing stimulus duration [4]. Temporal summation has been investigated for many years in tactile perception [59, 61, 62] and in other sensory modalities, especially in audition [63] and vision[64].

In 1960, Zwillocki proposed a mathematical model which was derived from the auditory psychophysical experiments, in which diverse temporal patterns of stimulus (e.g., repetition rate of multiple pulses, duration of tone bursts or multiple pulses and time interval between the pulses) were applied to measure auditory detection threshold [63]. The theory states that a neural excitation produced by a pulse or a single cycle of vibration shows an exponential decay with time. When stimulation has a proper timing pattern, a graded neural response produced by summation of resulting neural excitations occurs at the level of the temporal summator. This graded neural response controls the threshold as the timing pattern of stimulus changes, which constitutes the base of this theory [65]. The growth of summation with the increasing duration cause the energy integration. In the theory, an integrator which has a time constant of 200 ms is used to model the temporal summation. For a duration of 10 ms to 100 ms, the integration decreases the threshold at a rate of -3 dB/doubling of stimulus duration. On the other hand, for durations greater than 100 ms, there is an asymptotic decrease in threshold, which is completed at 1000 ms. Also, Zwillocki points out that stimulus frequency does not have an effect on the slope of integration.

It is proved that Zwillocki's model correctly predicts the slope of integration for any given temporal pattern of stimulus [63, 65, 66]. Verillo (1965) successfully apply the Zwillocki's model to the vibrotactile data. Verrillo found that temporal summation is observed when the large contactor (2.9 cm<sup>2</sup>) is used; however, there is an attenuation on temporal summation for the small contactor size (0.08 and 0.05 cm<sup>2</sup>) . He also stated that high frequency (>60 Hz) stimuli which affect Pacinian channel are summated over time and space, whereas energy of low frequency signals is not summated. When the low frequency stimuli which affect non-Pacinian channels are used, there is no difference between thresholds which are measured by small and large contactors. He also confirmed that the frequency does not change the slope of integration. The

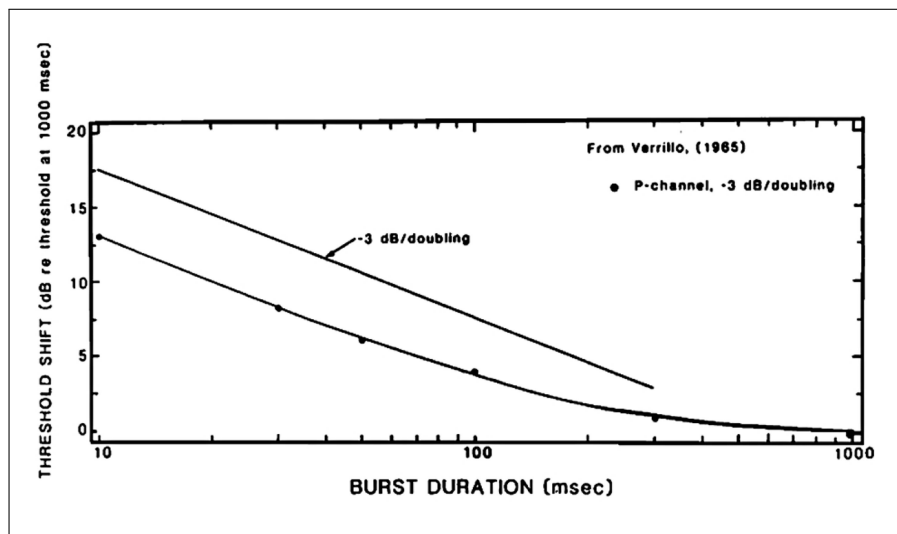


**Figure 2.8** The average results of Verrillo (1965) is replotted. The straight line indicates the slope of integration [63].

average results of Verrillo (1965) which shows relationship between the amplitude of signal elicited threshold and burst duration is replotted in figure 2.8. The upper line in the graph indicates the -3 dB/doubling slope in Zwislocki's model. According to the graph, the empirical data is consistent with the slope of integration [59].

Gescheider (1976) and Green (1976) also observed temporal summation when

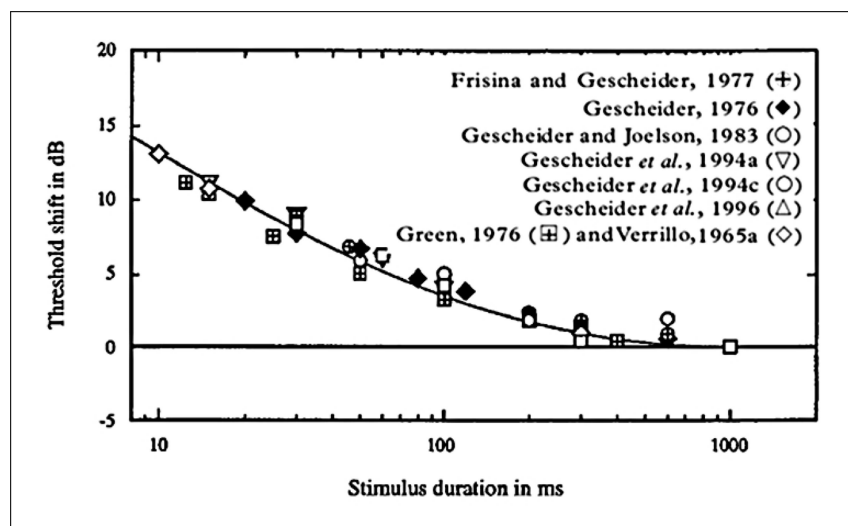


**Figure 2.9** Threshold shifts relative to detection threshold of 1000 ms in Pacinian channel from previous psychophysical studies. Solid function is adapted from Zwislocki's model [55, 59, 62, 63, 56, 67].

the high frequency vibrotactile stimuli are applied through a large contactor. However,

Green claimed that non-Pacinian channels have a small amount of temporal summation capacity at low frequency (25 Hz). He attributed the results that both Pacinian and non-Pacinian receptors contribute to detection of low frequency stimuli and that when stimulus duration increases, contribution of Pacinian channel increases too. Figure 2.9 shows the results of some of these studies as a function of threshold shift and stimulus duration. The straight function is adapted from Zwislocki's model. Also, figure 2.10 demonstrates the effects of duration on Pacinian and non-Pacinian channels.

From a physiological standpoint, it is assumed that the nervous system uses a code in order to represent events happened at the periphery. Because temporal integration occurs in the central nervous system [63] and contains temporal information of stimuli, the neural code at the periphery should also include the temporal information [61]. The peripheral code can be estimated by the means of integrating response of single nerve fiber and be plotted as a frequency-response function. In order to construct a frequency-response curve, an appropriate response criterion (e.g., entrainment, impulses/s and impulses/stimulus) should be determined. The criterion is generally

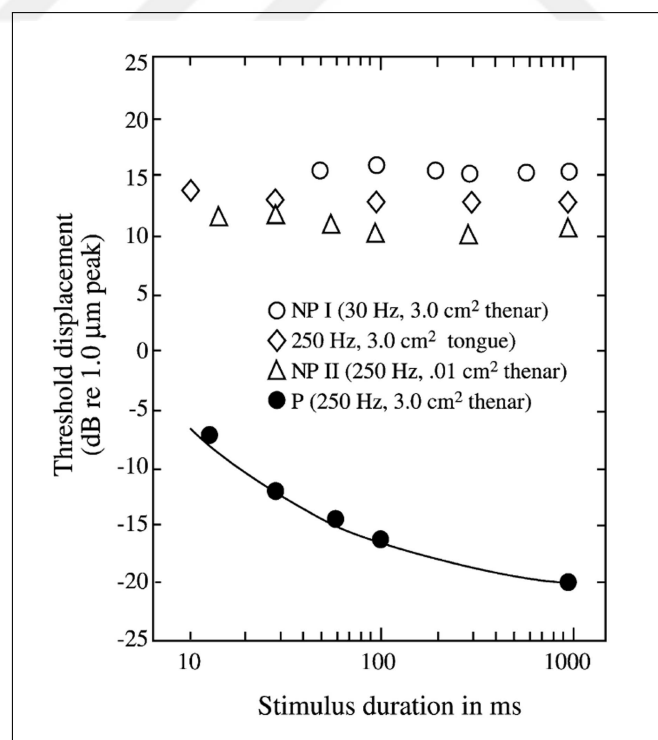


**Figure 2.10** The effect of stimulus duration on thresholds of Pacinian and non-Pacinian channels [4, 55, 56].

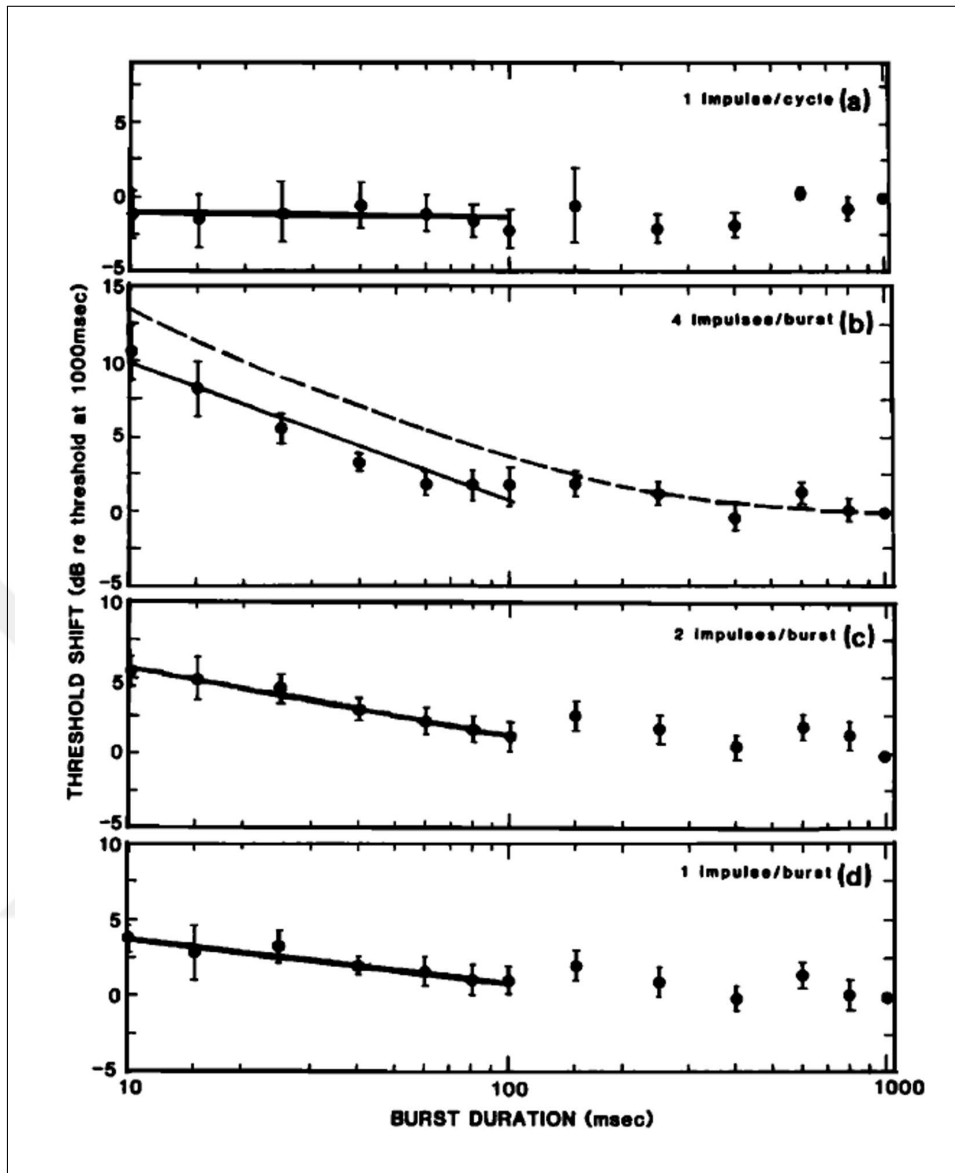


**Figure 2.11** The relationship between threshold shift relative to 1000ms and burst duration curve for four response criteria (1 impulse/cycle, 4 impulses/burst, 2 impulses/burst, 1 impulse/burst) [61].

selected according to the best correlation between physiological and psychophysical data. It is suggested that 2-4 neural impulses/stimulus which are emerged from single P afferent fiber are appropriate to determine the code of the threshold in the P channel [54].

In the study of Checkosky and Bolanowski (1992), the impact of the neural code was measured from single PCs at different stimulation durations. In order to obtain the response of integration, two techniques, ideal temporal integration and real-time temporal integration, were used. Ideal temporal integration is a method which adds



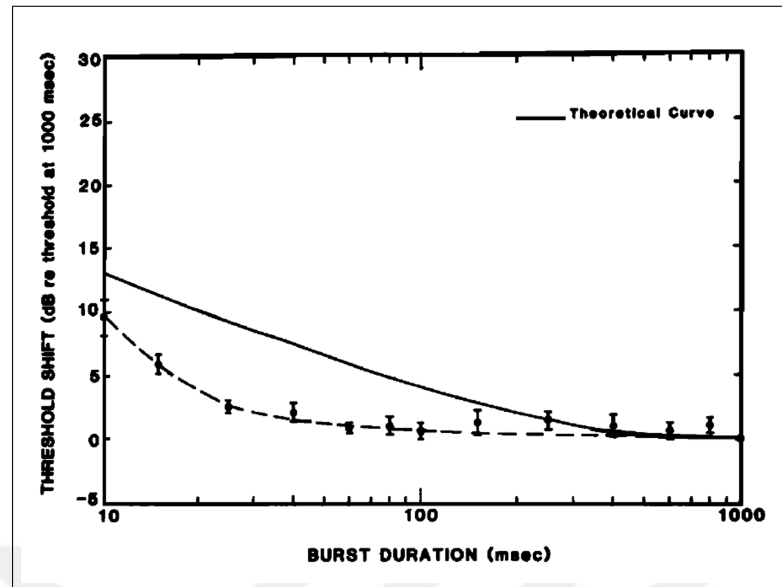


**Figure 2.12** Threshold shift curves obtained from theoretical model and temporal integrator with a 200 ms time constant [61].

up the number of neural responses over the duration of stimulation. It does not take into account when the responses to stimulation occurs. For four response criteria at 300 Hz, the relationship between threshold shift and stimulus duration was obtained by using ideal temporal integration method (figure 2.11). Among the four criteria, only 4 impulse/burst criteria approached the predicted temporal summation function; however, it still did not fully correspond to this function. On the other hand, real time integration was performed with temporal integrator with 200 ms time constant in order to model the central nervous system. The amplitude-duration function is acquired by using low-pass filter, but the function was not matched with psychophysical data (figure 2.12). It was concluded that the threshold of P channel is not sufficiently represented by single Pacinian nerve fiber.

Checkosky and Bolanowski (1994) compared three frequency response functions which are psychophysical frequency response of Pacinian channel of human subjects, physiological frequency response of human Pacinian fibers [68] and PCs isolated from cat mesentery [54]. (figure 2.13). All of them shows characteristic U-shape; however, they have many discrepancies stemming from different methodologies. Checkosky and Bolanowski stated that uncontrolled or diverse skin-surface temperature may cause the differences in the best frequency [69]. Another reason for the difference between the

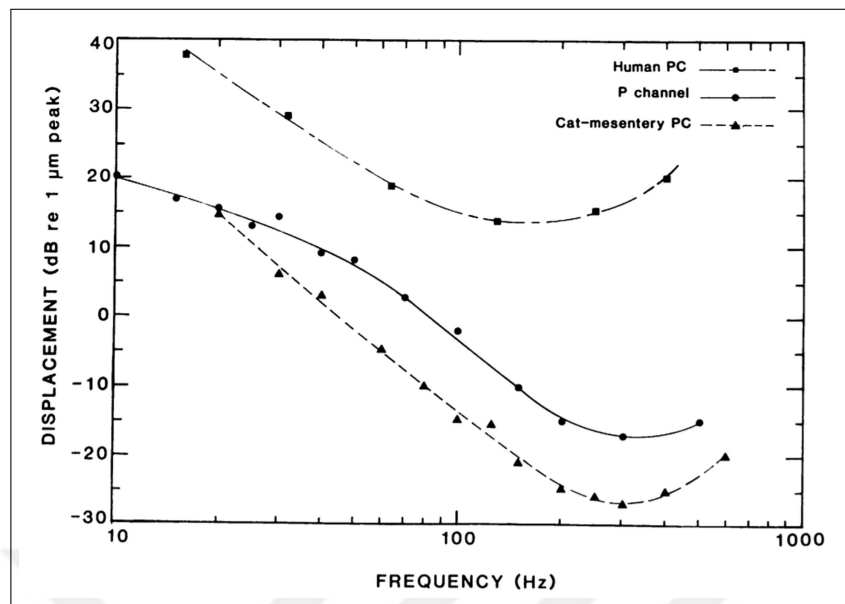


**Figure 2.13** Frequency-response curves of the human PC fibers, human P-channel and cat mesentery PC fibers [69].

human PC function and cat mesentery PC function could be that the most sensitive fibers were not stimulated. Furthermore, low frequency (50-150 Hz) slope of function for human subject (-9 dB/octave) is less steep than for cat mesentery PC and Pacinian channel (-12 dB/octave). Checkosky and Bolanowski (1994) performed psychophysical experiments on human subjects and physiological experiments on Pacinian corpuscles separated from cat mesentery in order to express these inconsistencies in the psychophysical-physiological model [54]. They benefited from Zwislocki's temporal summation model in order to predict slopes of frequency-response function. The function could be gathered with constant stimulus duration or constant numbers of stimulus cycle.

According to the theory, the curve of constant stimulus durations follows the Eq. 2.1, which defines the temporal integrator with time constant 200 ms. Threshold shift relative to detection threshold of 1000 ms is given in decibel units. Duration of stimulus is indicated with  $t$ . When the constant numbers of stimulus cycle are used, the curve obeys the Eq. 2.2.  $n$  is the number of cycles, which occur over stimulus duration ( $t$ ) with period ( $T$ ). Also,  $v$  is the frequency of stimulus which equals the  $1/T$ .

$$TS = -10 \log(1 - e^{-5t}) \quad (2.1)$$

$$TS = -10 \log(1 - e^{-5\frac{n}{v}}) \quad (2.2)$$

In the study of Checkosky and Bolanowski (1994), both experimental psychophysical and physiological results obtained by constant duration and constant number of stimulus cycle method were consistent with Zwislocki's theory (1960). The group means slopes of two methods are statistically different from each other. Also, 5 cycle curve has a greater sensitivity than constant duration curve, because of static indentation level (figure 2.14).

Also, there is another study (Gescheider et al. 2002) which compares the temporal summation mechanisms at the fingertip and thenar eminence. It stated that the interaction of testing site does not affect threshold shift relative to 1000 ms for detection of 300 Hz stimuli (figure 2.15) [60].

Apart from the Zwislocki's neural integration theory, probability summation theory is used to explain temporal summation mechanism. According to probability summation theory, a long stimulus has a more chance to produce a neural response which decreases the psychophysical threshold [70].

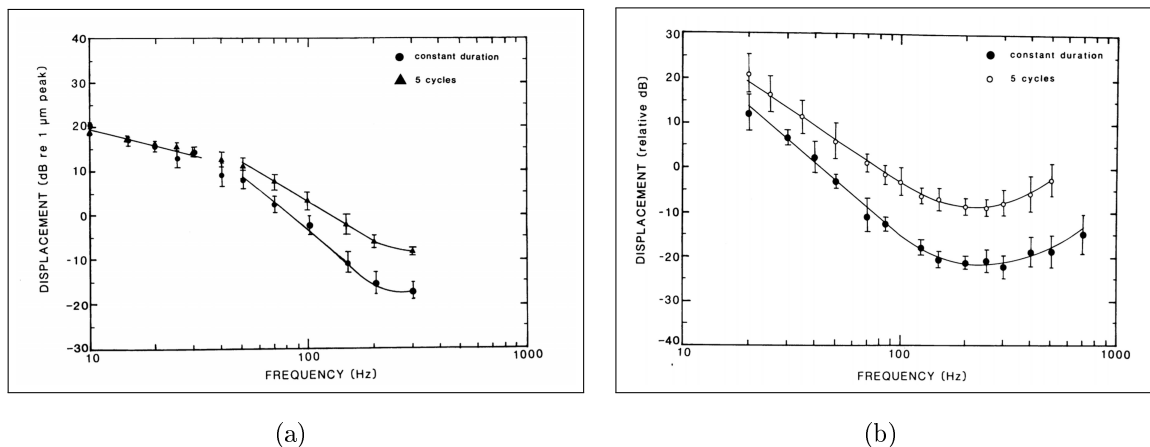


**Figure 2.14** The frequency response curves obtained with constant duration and constant cycles. a) The curve was obtained from P-channel. b) The curve was obtained from PCs isolated from cat mesentery [69].

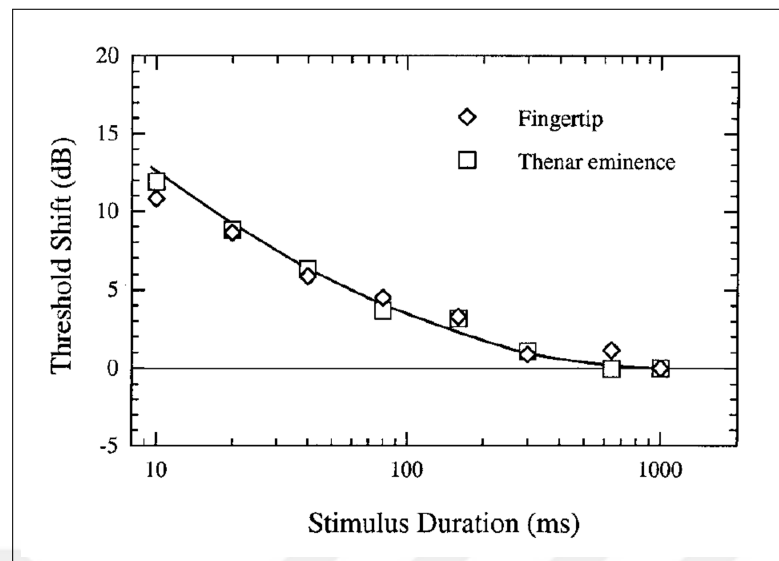


**Figure 2.15** Threshold shift relative to detection threshold of 1000 ms in thenar eminence and fingertip [60].

Yıldız et al. (2011) conducted preliminary psychophysical experiments based on fast adaptive tracking method and showed that temporal summation of Pacinian channel is independent of frequency. There was a 6.6 dB difference in threshold between 10 ms and 1000 ms stimulation observed.

However these previous studies were obtained only one point in the psychometric curve. In this study, six different data points measured with method of constant stimuli in order to plot psychometric function in detailed way. Therefore, both slope and midpoints (threshold) of the curve gave information about the temporal summation mechanism.

## 3. METHODOLOGY

### 3.1 Subjects

Four male and six voluntary female (ages: 25-30) subjects took part in this study. Two of the subjects were left-handed and rest were right-handed. The study was approved by Ethics Committee for Human Subjects of Boğaziçi University. All subjects signed the consent form. Participants who did not have any neurological disorders and dermatological problems were chosen to avoid affecting the results.

### 3.2 Apparatus

The apparatus resembled the one which was used by Güçlü and Öztekin (2007). The experiment was conducted in a sound and vibration proof room. The stimulus waveform was generated in the computer which had a connection with a digital-to-analog converter card (DaqBoard/2000, IOtech, Cleveland, OH). After the stimulus level was altered by a PA5 digital attenuator (Tucker-Davis Technologies, Alachua, FL), the signal was conveyed to an RA300 power amplifier (Alesis, Fort Lauderdale, FL) to drive the mechanical shaker. Displacements of the shaker was monitored by a Schaevits ATA2001 LVDT (Lucas Control Systems, Pennsauken, NJ) and a TDS 2014 digital oscilloscope (Tektronix, Inc., Beaverton, OR). The shaker was calibrated by a fotonic sensor (MTI-2100, MTI Instruments, Albany, NY, USA) (figure 3.1- 3.2).

A cylindrical probe ( $r = 2 \text{ mm}$  and  $\text{area} = 0.126 \text{ cm}^2$ ) was used to apply stimulus. In order to prevent the movement, the left middle finger of the subject was fixated by modelling clay (figure 3.3). Also, the position of finger was monitored by a charged coupled camera. Since the Pacinian channel is influenced by temperature [42], surface temperature of the left middle finger was measured by thermometer probe which was connected to a multimeter. The average temperature was 32-34 °C, so

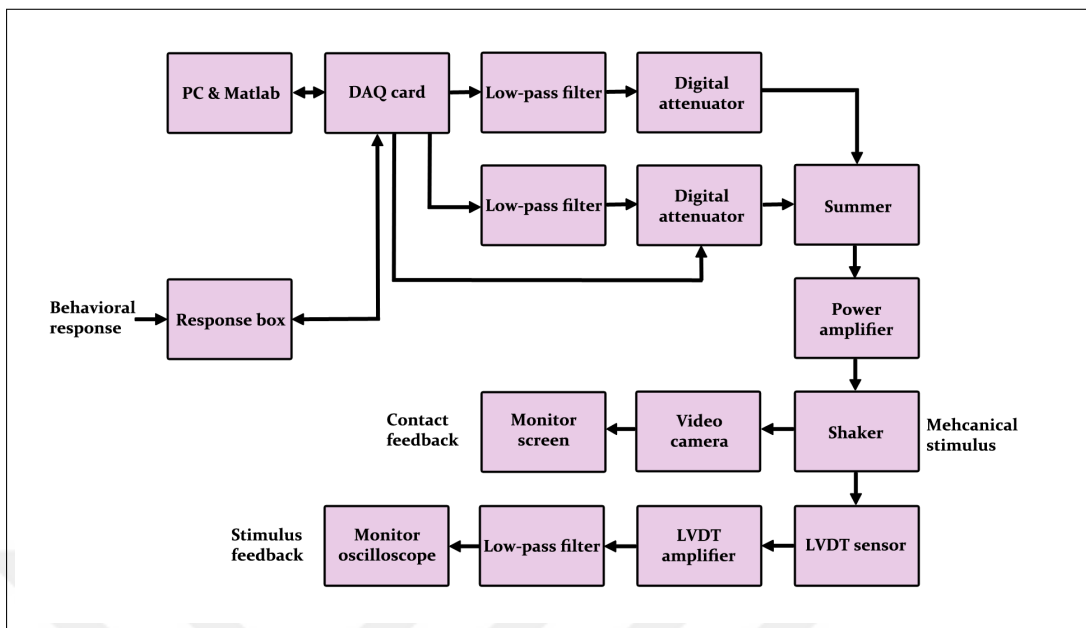


**Figure 3.1** Block diagram of the experimental setup



(a)

(b)

**Figure 3.2** (a) Experimental setup (b) isolated room.

the narrow temperature range did not affect the threshold of the Pacinian channel. Participants gave their response via a response box that included buttons and LEDs to cue the stimulus intervals with light. During the experiment, subjects wore headphones which presented white noise to prevent hearing sound emitted from the shaker at high frequencies.

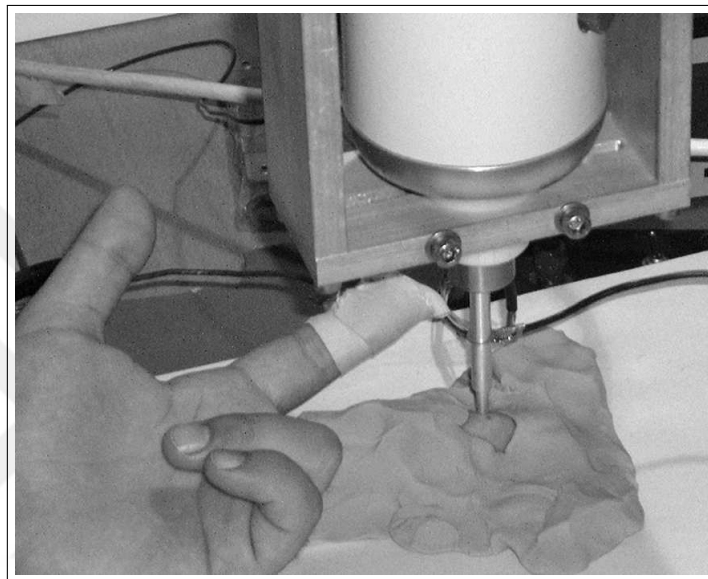


**Figure 3.3** Shaker and hand position of the experiment [71].

### 3.3 Stimuli

In the experiment, bursts of sine waves were used as stimuli which were superimposed on a 0.5 mm static indentation. The stimuli had 10 ms rise and fall times that were formed in cosine-squared ramps (figure 3.4). The test stimuli were presented at six different frequencies: 100, 150, 250, 350, 500 and 750 Hz and at five different durations (d) that were 10, 30, 100, 300 and 1000 ms.

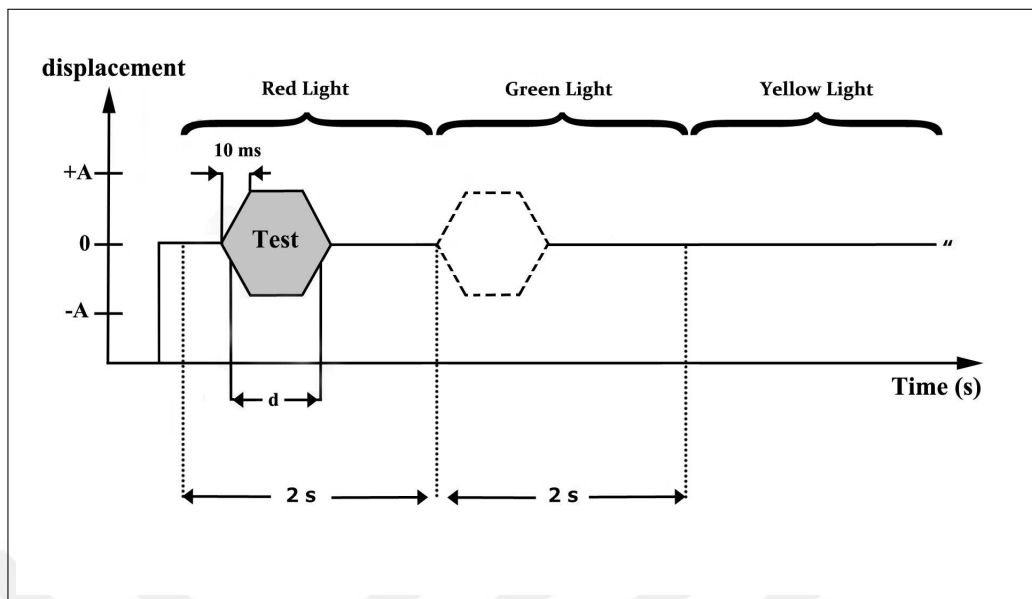


Figure 3.4 Timing diagram of experiment.

### 3.4 Procedure

In the experiment, first, an adaptive tracking method was used to measure detection threshold of each participant. The stimuli were presented in a two-interval forced choice tracking task. The participants were instructed to select the interval in which they detected the vibrotactile stimulus. The intervals were cued by red and green light. The participants gave their responses during the indication of yellow light. The amplitude of stimulus increased 1 dB for each incorrect response and decreased 1 dB for three correct responses (not necessarily consecutive), which is referred as up and down rule. When the stimulus level was steady within  $\pm 1$  dB range for last 20 trials, the program automatically stopped the experiment. This method measured threshold at the 0.75 correct probability of detection [31]. For each condition (frequency and duration combination), measurement of detection threshold was completed.

In order to obtain the psychometric functions, the method of constant stimuli was used in a similar two interval forced choice task. For this purpose, six different amplitudes of stimuli with 40 repetitions were randomly presented at each condition (frequency and duration combinations). Three amplitude values were selected above the detection threshold of subject ( $Th+2$ ,  $Th+4$ ,  $Th+6$  in dB), one at threshold ( $Th$  in dB) and two below the threshold ( $Th-2$ ,  $Th-4$  in dB). The conditions consisted of



every combination of six different frequencies (100, 150, 250, 350, 500, and 750 ms) and five durations (10, 30, 60, 300 and 1000 ms).

### 3.5 Data Analysis

The results of each condition (frequency and duration combinations) were plotted as a psychometric function which indicates the relationship between probability of correct responses and intensity level of stimulus. The data points were fitted by sigmoidal curves with nonlinear regression using Eq. 3.1.

$$p_c = 0.5 + \frac{0.5}{(1 + e^{\frac{-(x-\alpha)}{\beta}})} \quad (3.1)$$

According to the Eq. 3.1,  $x$  is the amplitude of the stimuli in unit of  $\mu\text{m}$ .  $\alpha$  is the midpoint of the curve which corresponds to 75% detection probability, and is defined as the psychophysical threshold given in unit of  $\mu\text{m}$ . Also, *beta* ( $\beta$ ) is a parameter which is related to slope ( $1/8\beta$ ) of the psychometric function at  $\alpha$ . For each condition, goodness of fit of the psychometric function was measured.

Threshold and slope values were used in statistical tests. First, aligned rank transform was performed on data because of the small sample size. Then, rank data was analyzed with repeated measures ANOVA, in which the effects of frequency, duration and their interaction were studied.

## 4. RESULTS

### 4.1 Psychometric Functions

Ten subjects completed the psychophysical experiments in which method of constant stimuli was used. For each duration-frequency condition (30 conditions), the probability of correct detection of subjects at each amplitude was measured. At each condition, the data were fitted by the sigmoidal curve with nonlinear regression in order to obtain psychometric curves which are shown in figure 4.1-4.6.  $R^2$  (goodness of fit) values of 273 psychometric functions out of 300 were higher than 0.70 and the rest of them were between 0.57 and 0.70. The conditions which gave  $R^2 < .70$  were not used in subsequent analysis for each subject. Also, average  $R^2$  of all data was 0.88.

Midpoints of psychometric curves ( $\alpha$ ) which correspond to 75% detection probability threshold and slopes ( $1/8\beta$ ) calculated from the psychometric functions for all conditions (table 4.1-4.2). Then, outlier analysis (Peirce's criterion) was performed to eliminate outlier data. The outlier data were replaced with the average of subjects for that condition. Following that, aligned rank transform was applied on the thresholds and slopes in order to use a parametric statistical test.

**Table 4.1**

Averages of threshold and slope values which were obtained from psychometric function for 100 Hz.

Frequency (Hz)	Duration (ms)	Threshold ( $\alpha$ )	Slope ( $1/8\beta$ )
100	10	4.6618	0.1489
100	30	2.3528	0.3692
100	100	1.7145	0.2778
100	300	1.6922	0.3640
100	1000	1.6782	1.1385

**Table 4.2**  
Averages of threshold and slope values which were obtained from psychometric function for 150, 250, 350, 500 and 750 Hz.

Frequency (Hz)	Duration (ms)	Threshold ( $\alpha$ )	Slope ( $1/8\beta$ )
150	10	2.0768	0.2749
150	30	1.4276	0.8022
150	100	1.0179	0.5958
150	300	0.8797	0.5964
150	1000	0.5771	0.9972
250	10	1.2441	0.4905
250	30	0.9838	0.8366
250	100	0.6722	1.2057
250	300	0.4507	1.3150
250	1000	0.5443	1.9924
350	10	1.1488	0.6050
350	30	0.9188	0.8703
350	100	0.5146	1.3336
350	300	0.4280	1.6881
350	1000	0.4173	2.4594
500	10	1.4080	0.3578
500	30	1.1436	2.5604
500	100	0.9964	1.3100
500	300	0.8784	0.7051
500	1000	0.5834	1.3477
750	10	1.9346	1.2242
750	30	1.7059	0.5487
750	100	1.7255	4.5481
750	300	1.3438	0.6281
750	1000	1.0523	0.5729

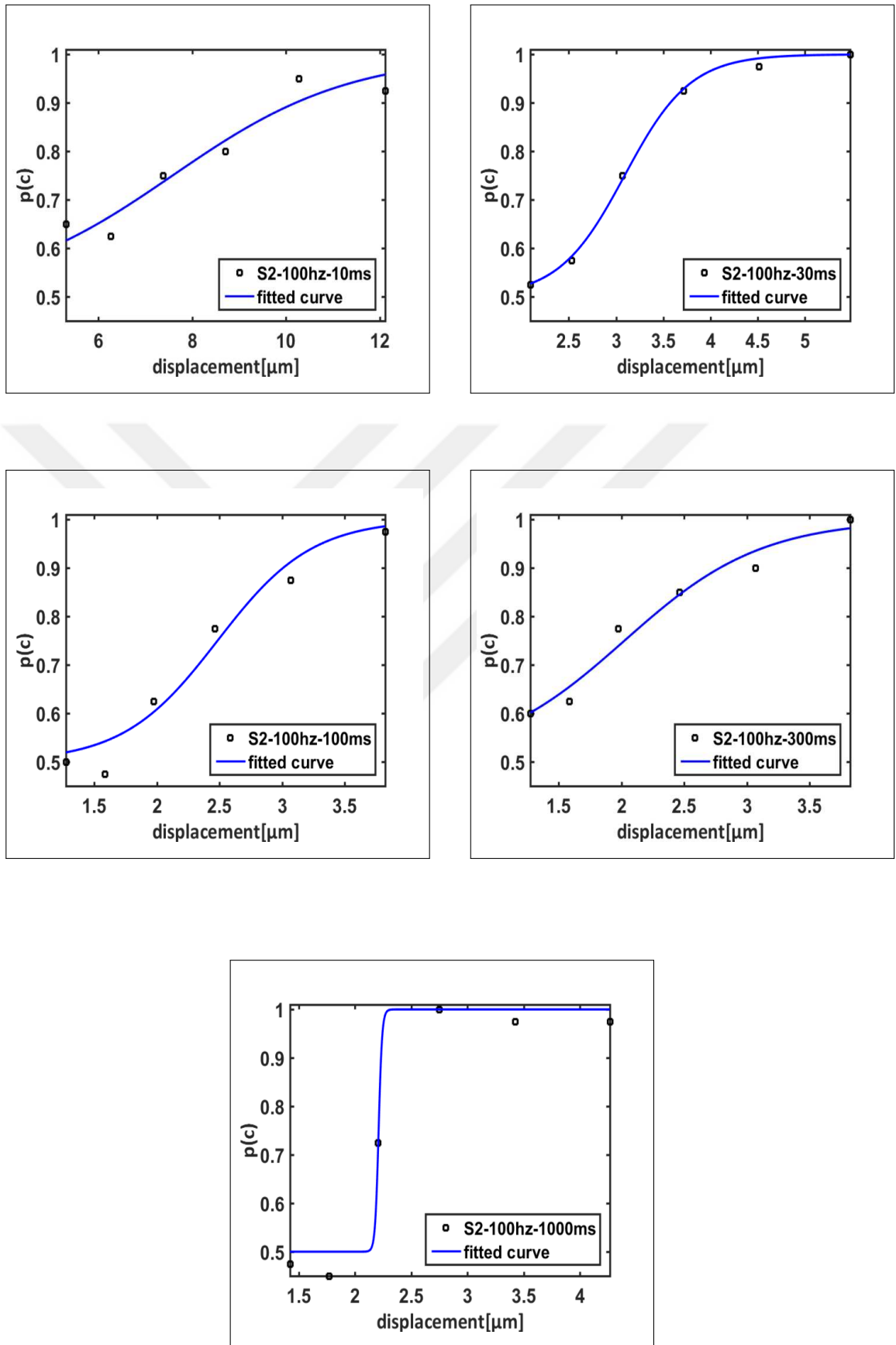


**Figure 4.1** Psychometric curves of subject-2 at 100 Hz for all durations. ( $p(c)$  is the probability of correct detection.)

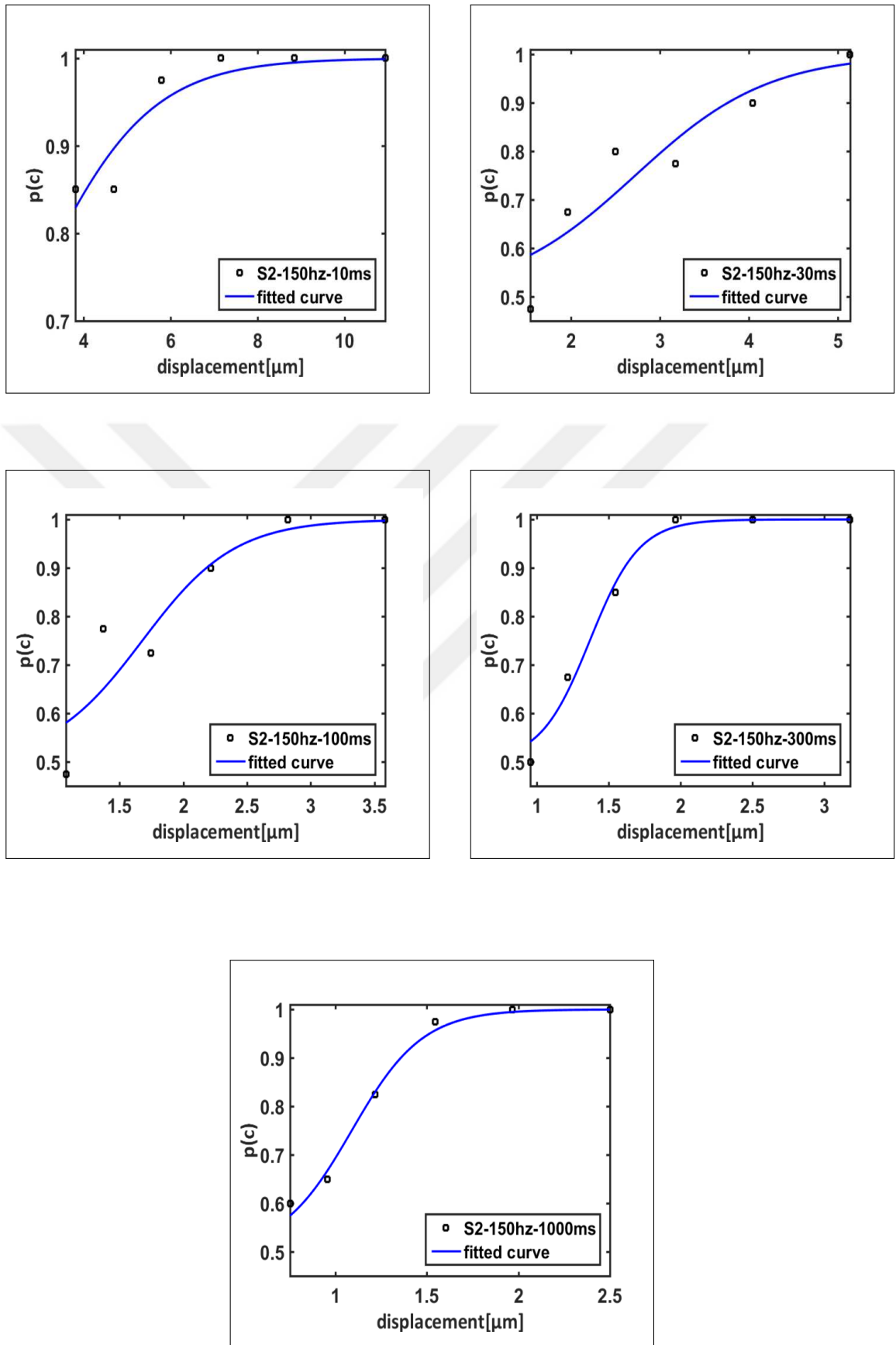


**Figure 4.2** Psychometric curves of subject-2 at 150 Hz for all durations. ( $p(c)$  is the probability of correct detection.)

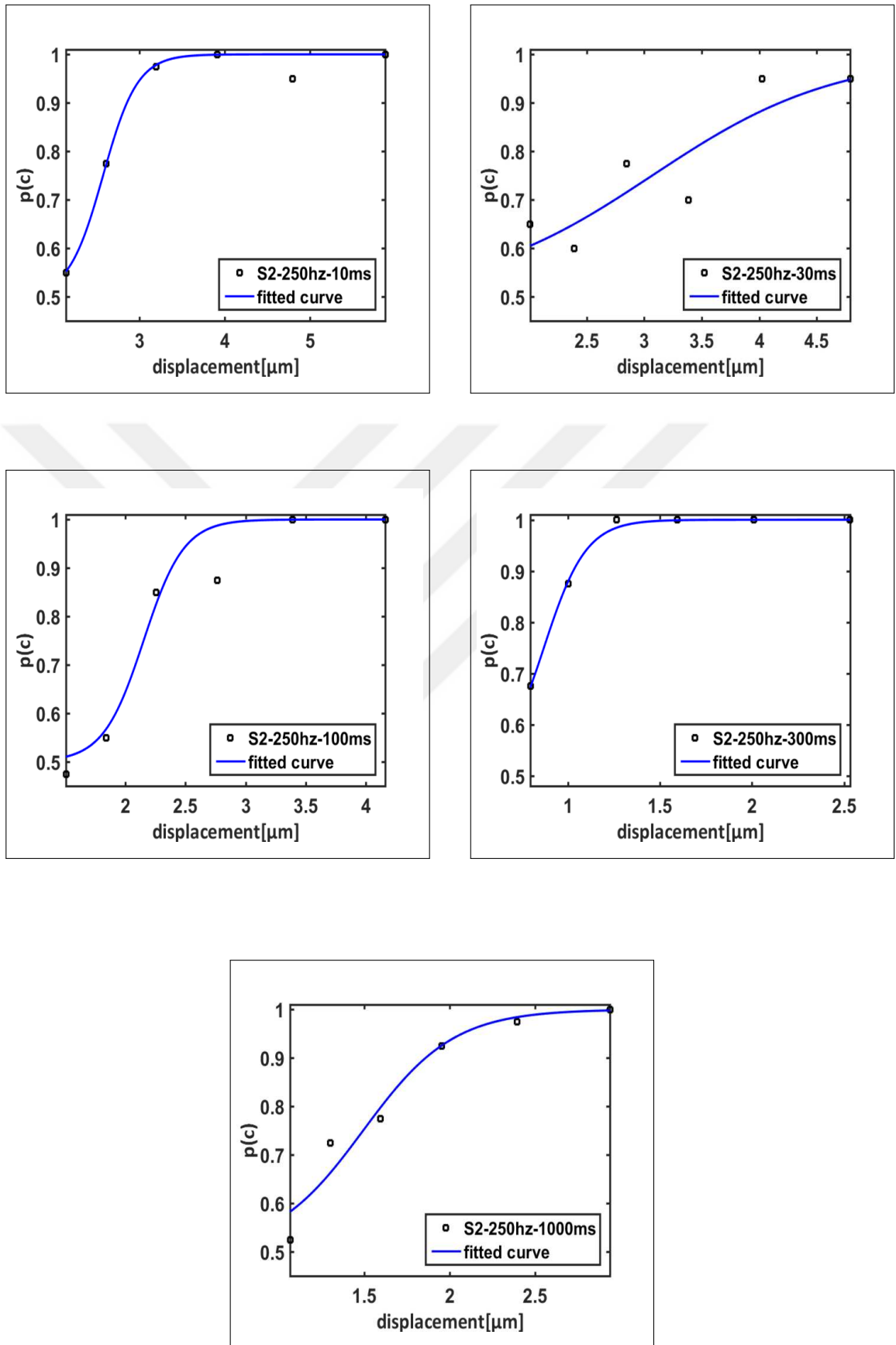


**Figure 4.3** Psychometric curves of subject-2 at 250 Hz for all durations. ( $p(c)$  is the probability of correct detection.)

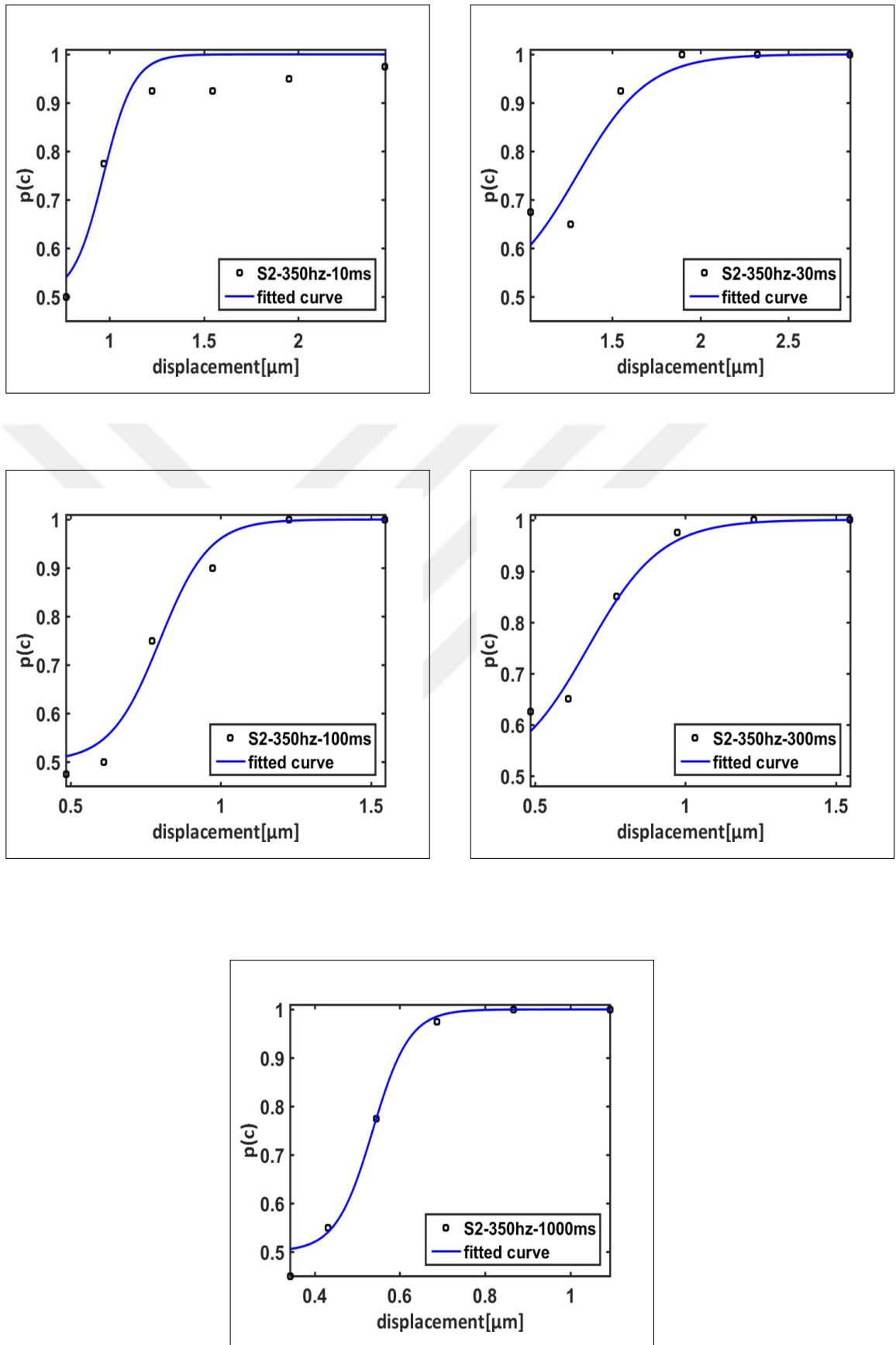


**Figure 4.4** Psychometric curves of subject-2 at 350 Hz for all durations. ( $p(c)$  is the probability of correct detection.)

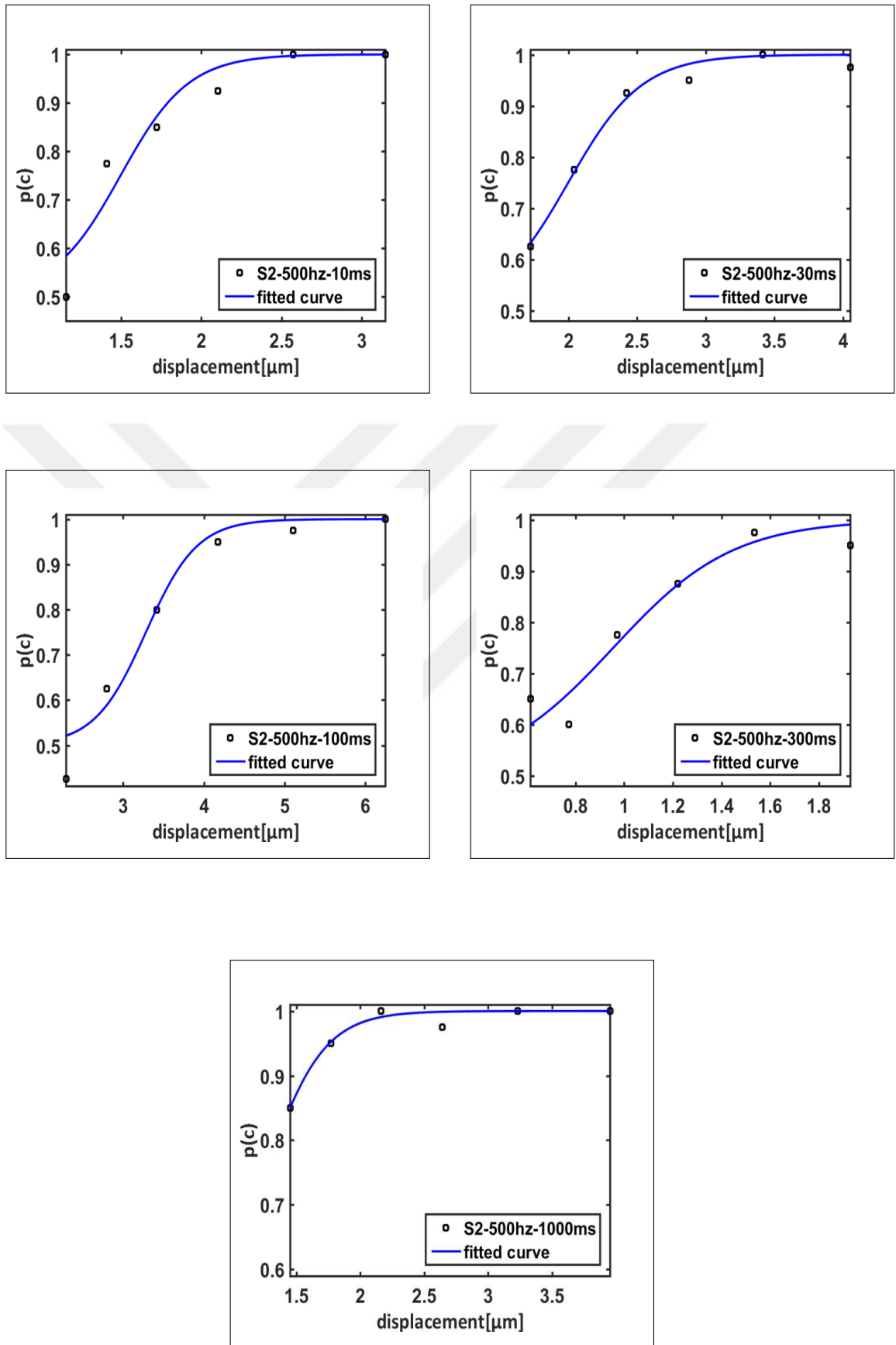


**Figure 4.5** Psychometric curves of subject-2 at 500 Hz for all durations. ( $p(c)$  is the probability of correct detection.)



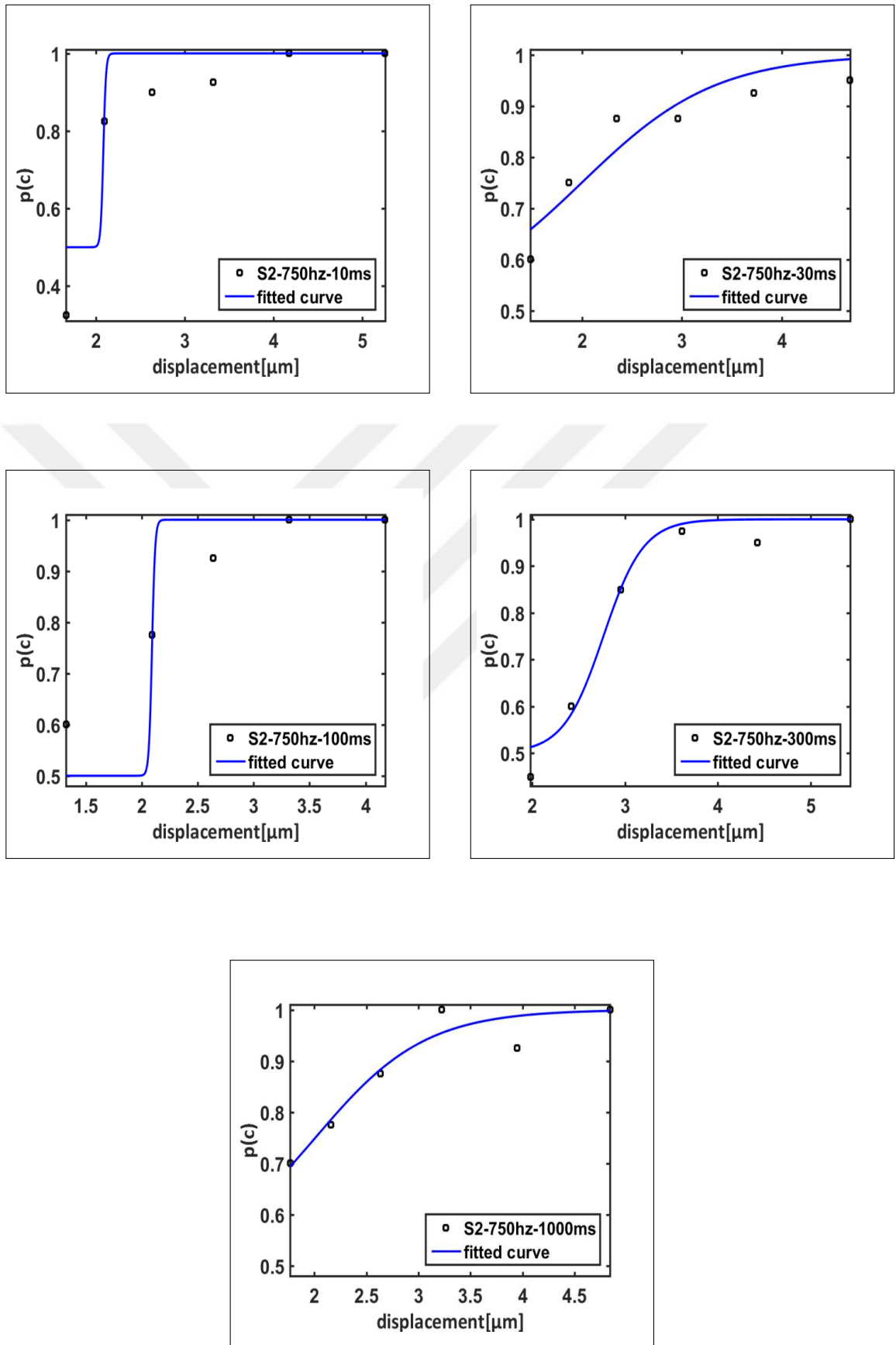


**Figure 4.6** Psychometric curves of subject-2 at 750 Hz for all durations. ( $p(c)$  is the probability of correct detection.)

## 4.2 Effects of Frequency on Temporal Summation

Duration effects on frequency-threshold ( $\alpha$ ) curve of ten subjects are shown in figure 4.7. It was observed that frequency-response curves shifted down, as durations increased. Also, the characteristic U-shape of the channel was evident for each curve. In addition, all subjects' average thresholds and slopes were plotted as frequency-response curves in figure 4.8-4.9.

The effect of frequency, duration and interaction between them were analyzed with the repeated measures ANOVA. Threshold of Pacinian channel ( $\alpha$ ) changed with frequency that was consistent with the previous studies and maintained the characteristic U-shape ( $F(5,45) = 42.50$ ,  $p < 0.001$ ). The displacement values of most sensitive part of the frequency-response curves were  $1.15 \mu\text{m}$  for 10 ms,  $0.92 \mu\text{m}$  for 30 ms,  $0.52 \mu\text{m}$  for 100 ms,  $0.43 \mu\text{m}$  for 300 ms and  $0.42 \mu\text{m}$  for 1000 ms at 350 Hz. Also, when the duration increased, a statistically significant decrease in threshold ( $\alpha$ ) was observed ( $F(4,36) = 60.34$ ,  $p < 0.001$ ). However, an interaction between the frequency and duration was not found in thresholds ( $F(1,9) = 4.84$ ,  $p = 0.055$ ). This shows that temporal summation was not significantly affected by frequency change in the Pacinian channel.

Likewise, frequency had a main effect on the slope; however, interestingly, the shape of frequency-response curve was similar to an inverted U-shape ( $F(5,45) = 29.64$ ,  $p < 0.001$ ). At 350 Hz, the slope of the curves were  $0.61 \text{ 1}/\mu\text{m}$  for 10 ms,  $0.87 \text{ 1}/\mu\text{m}$  for 30 ms,  $4.55 \text{ 1}/\mu\text{m}$  for 100 ms,  $1.68 \text{ 1}/\mu\text{m}$  for 300 ms and  $2.46 \text{ 1}/\mu\text{m}$  for 1000 ms. Also, the slope increased as the duration increased for all frequencies but 750 Hz ( $F(4,36) = 26.58$ ,  $p < 0.001$ ). Similarly, there was indeed an interaction between frequency and duration in the slopes ( $F(20,180) = 3.85$ ,  $p < 0.001$ ).

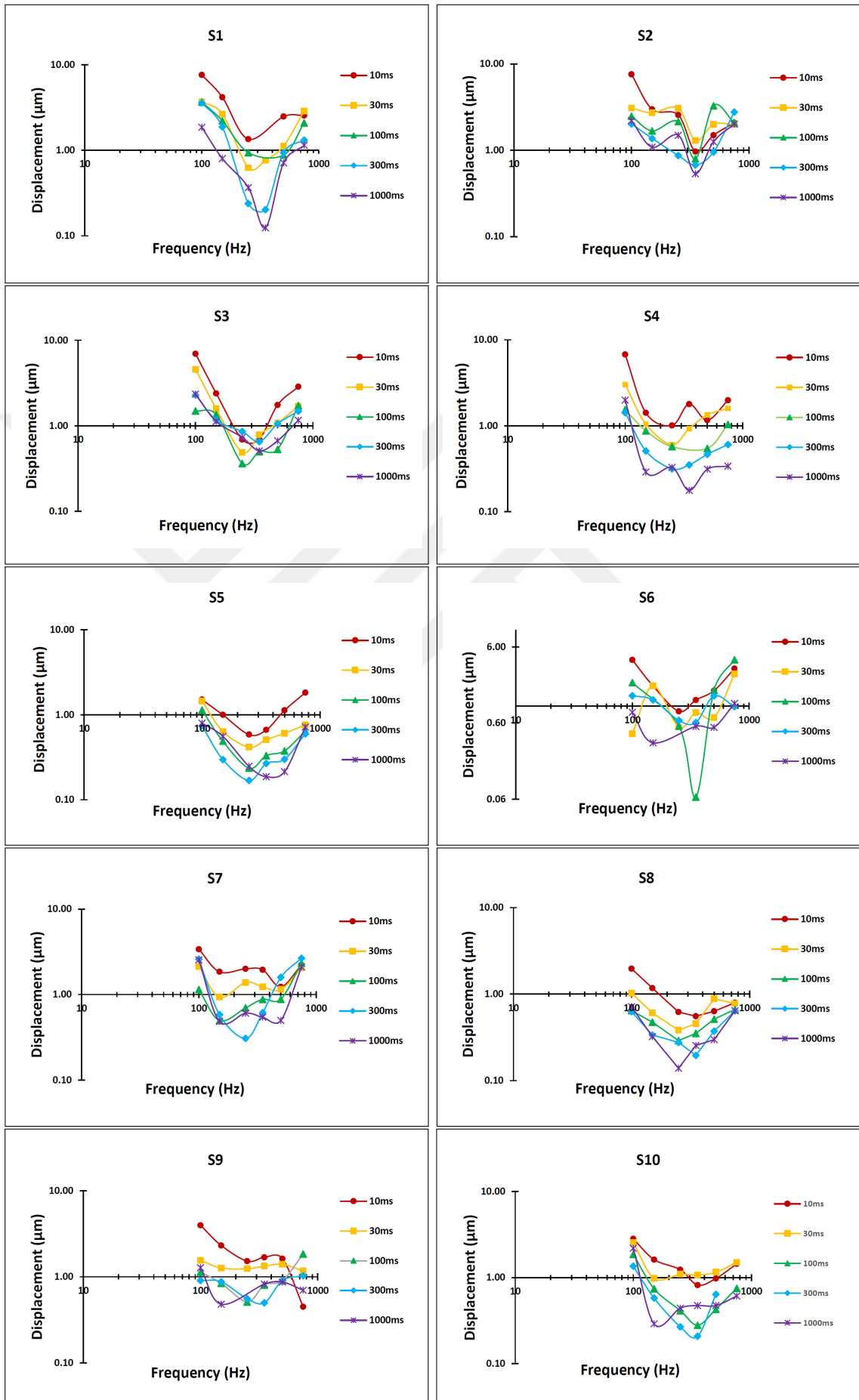
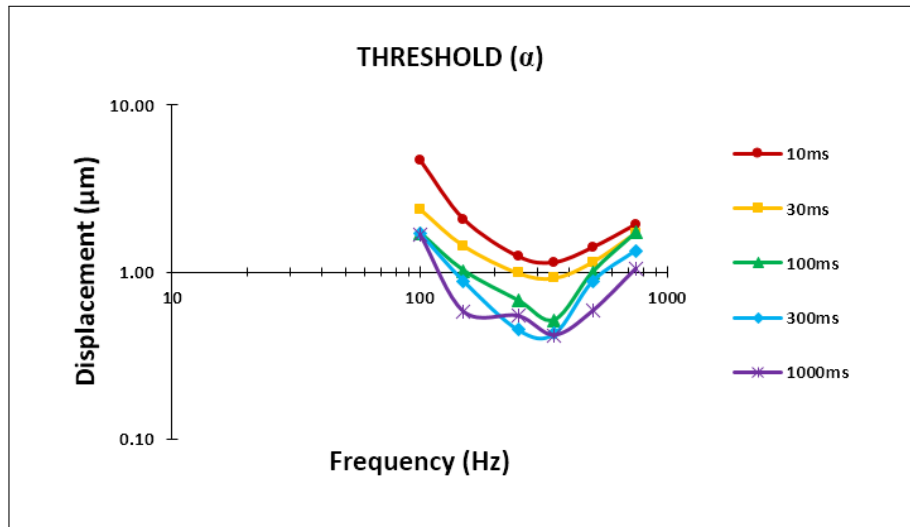
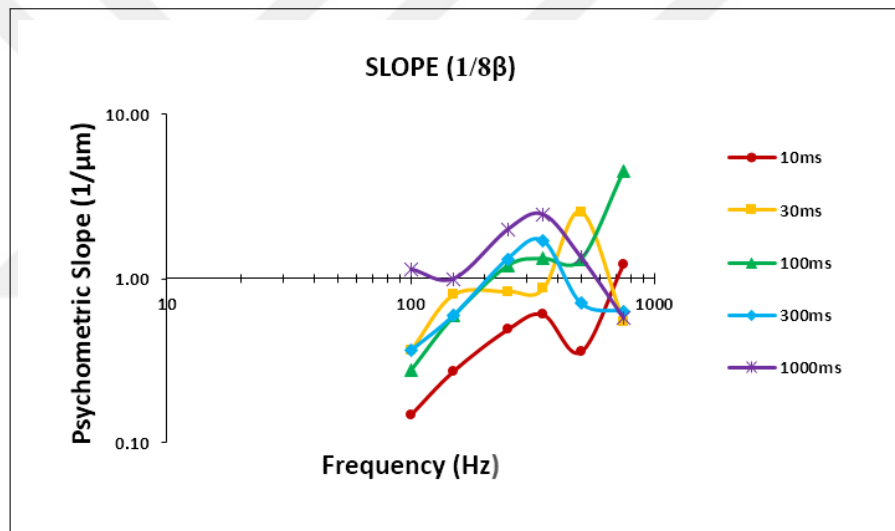


Figure 4.7 Frequency-threshold curves of 10 subjects for all durations.



**Figure 4.8** The relationship between displacement ( $\alpha$ ) and frequency for all durations.



**Figure 4.9** The relationship between psychometric slope ( $1/8\beta$ ) and frequency for all durations.

### 4.3 Threshold Shift

Average threshold shift (dB) relative to threshold of 1000 ms was calculated from the data in figure 4.8. Threshold shifts are plotted as a function of duration for each frequency ( $dBShift = 20 \log (threshold/threshold_{1000})$ ) (Figure 4.3). For 100 Hz, 150 Hz, 250 Hz, 500 Hz and 750 Hz, threshold shift between 10 ms and 1000 ms was respectively 8.87, 11.12, 7.18, 8.8, 7.65 and 5.29 dB.

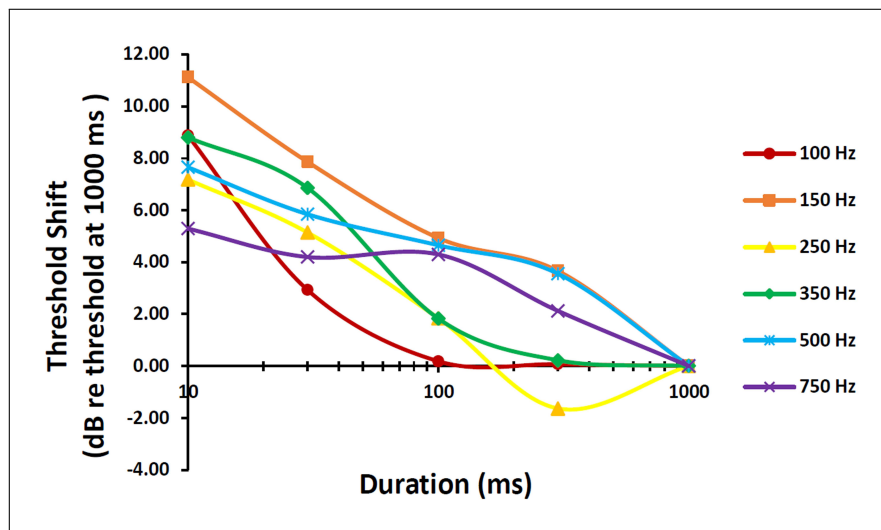


**Figure 4.10** The relationship of average threshold shift relative to 1000 ms and duration.

Threshold (dB re  $1\mu\text{m}$ ) decrease per doubling of stimulus duration (slope of the threshold shift) between 10 ms and 100 ms was calculated for each frequency by fitting a straight line through the data points in figure . Table 4.3 shows these slopes (dB shift/doubling of duration). The results were not very different from the Zwillocki's temporal summation theory which predicted from the -3 dB per doubling.

**Table 4.3**

Threshold decrease per doubling of stimulus duration between 10 ms and 100 ms for each frequency.

Frequency (Hz)	dB shift/doubling of duration
100	-2.60
150	-1.86
250	-1.61
350	-2.11
500	-0.90
750	-0.29

## 5. DISCUSSION

Effects of frequency on temporal summation in the Pacinian corpuscle was investigated with psychophysical experiments in this thesis. More detailed information about the temporal summation mechanism was gathered by using the method of constant stimuli. Then, psychometric functions were obtained, which provided the essential data for psychophysics including the relationship between stimulus strength and probability of correct detection of subject response.

### 5.1 Effects of Frequency on Threshold and Slope of Psychometric Function

When the thresholds ( $\alpha$ ) obtained from psychometric curves were plotted as a function of frequency, characteristic U-shape of Pacinian corpuscle was obtained for all durations (figure 4.8). According to previous studies, the lowest threshold was seen at the range of 250-300 Hz in the frequency-response curve of Pacinian channel [57]. Similarly, the results of this experiment verified that the most sensitive part (approximately  $1.15 \mu\text{m}$  for 10 ms,  $0.92 \mu\text{m}$  for 30 ms,  $0.52 \mu\text{m}$  for 100 ms,  $0.43 \mu\text{m}$  for 300 ms and  $0.42 \mu\text{m}$  for 1000 ms ) of U-shape portion was found at 350 Hz for all durations.

The slope is a parameter which has an inverse relationship with the threshold variance. The slope of psychometric function provides an advantage in comparing thresholds that are gathered with different criteria across empirical studies. Also, steepness of slope can be used as a parameter in order to obtain information about reliability of estimation of sensory threshold [72]. In our study, frequency had a main effect on the slope of psychometric functions for all durations. The slope-frequency curves had an inverted U-shape which have the highest point between the 250 Hz and 350 Hz portion. It seems that the frequencies which result in lowest thresholds have highest slopes [73]. Further investigations are required to study the inverse relationship between threshold

and slope as a function of frequency and duration. It is also interesting to note that stimulus duration increased, slopes shifted upwards.

## 5.2 Temporal Summation in Pacinian Channel

According to the Zwillocki's theory [63], it is expected that increasing stimulus duration causes a decrease in detection threshold. In this experiment, temporal summation effect occurred at six different frequencies. The theory suggests that when the duration is between 10 and 100 ms, there is a decrease in threshold at a rate of -3 dB/doubling of stimulus duration. However, for duration 100 ms to 1000 ms, an asymptotic decrease in threshold is observed and is completed at 1000 ms. In this study, experimental data had a threshold decrease at -2.60, -1.61, -2.11, -0.90, -0.29 dB/doubling of duration for 100, 150, 250, 350, 500 and 750 Hz, respectively. At 100 and 350 Hz, the threshold decreases were consistent with the previous studies. The reason of different behavior of 500 and 750 Hz curves is unknown, so it needs further examination. Also, an asymptotic decrease which is stated in the model was shown only at 100 Hz and 150 Hz for duration higher than 100 ms.

In previous studies, the total threshold shift between 10-1000 ms was 12 dB at 100 Hz [59], 15 dB at 160 Hz [4] and 13 dB at 300 Hz [60]. However, we found that the threshold shift was nearly 8 dB for all frequencies except 150 Hz which had 11 dB shift. This difference may be stemming from experimental conditions related to the size of stimulus contactor and using a contactor surround. Gescheider et al. (1978) showed that when the contactor surround was used in the psychophysical experiments, threshold increased approximately 10 dB compared to the threshold obtained without contactor [74]. This difference may affect the temporal summation mechanism. Also, using large contactor area increases the spatial summation of Pacinian channel, which decreases the detection threshold [60]. In the previous studies, contactor sizes were larger than this study, so this may cause the difference of threshold shift.

Another finding about the temporal summation mechanism was that the slope of psychometric curves gave information about the stimulus duration for all frequencies

but 750 Hz. The reason of this may also be the relationship between the threshold and slope [73]. There is no previous study related to temporal integration in slopes of the psychometric curve, so this is one of the novelty of this study.

In the study of Gescheider et al. (2005), psychometric curves were obtained using different contactor size (between 0.05, 0.38, 0.75, and 1.5 cm<sup>2</sup>) and durations (0.1 and 1 s) at thenar eminence with rigid surround. There was only 3-4 dB threshold shift between the 0.1 and 1 s for 300 Hz (not statistically significant) [75]. Our results are consistent with their results. We found 1.82 dB threshold shift between 0.1 s and 1 s occurred for 350 Hz. However, the slope of the psychometric curve was not much affected by duration change in their study which is somewhat contradictory to our results. This may be the result of the large contactor sizes used in their study.

Güçlü et. al (2005) applied a population-response model to psychophysical data of Gescheider et al. (2005) in order to predict effects of spaital summation (figure 5.1). Additionally, some temporal summation was also observed in that model [76]. In simulation, approximately 6.9 dB threshold shift occurred between 2-1000 ms for both contactor sizes (0.05 and 1.5 cm<sup>2</sup>). Typically more temporal summation is expected from such a large duration difference. Therefore, the model should be revised to include the mechanism of temporal summation. The model also predicted smaller slopes for the dB shift for the larger contactor.

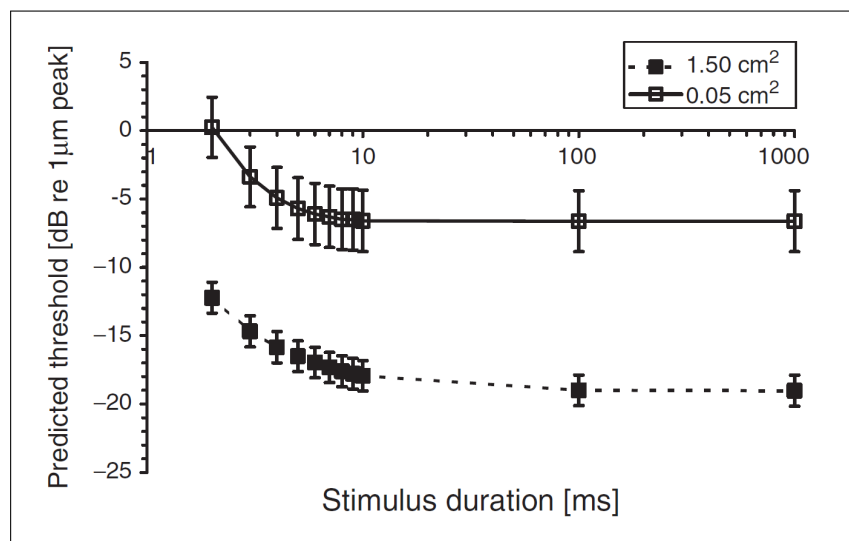


**Figure 5.1** Temporal summation for two different cotactor sizes in the constant population model [76].



Apart from the neural integration theory, there is a probability summation theory which has an effect on temporal summation. It states that individual fibers have different sensitivities. At longer durations, the probability of production of neural responses increases. Also, when a large contactor is used, a chance of the activation of the most sensitive fibers increases [57]. Therefore, contactor size may have caused some of the differences which are stated in this study compared to previous work.

### **5.3 Effects of Frequency on Temporal Summation**

Zwislocki (1960) stated that frequency does not affect the slope of integration in temporal summation. Verrillo (1965) applied the Zwislocki's temporal summation theory on the tactile psychophysical experiments and verified that the slope of integration in the Pacinian channel is independent of frequency. By using a method similar to previous work Yıldız et al. (2011) obtained results consistent with Zwislocki's theory. Most of the previous studies related to this issue were conducted based on fast adaptive tracking method, whereas method of constant stimuli which provides more detailed information was used in the current study. The slope of psychometric function and threshold values provided a consistent picture of temporal summation. It was found that increasing duration had robust effects on thresholds and psychometric slopes. As a matter of fact, the change of thresholds were almost constant at different frequencies tested for the Pacinian channel. Therefore, the results of this thesis further supports the concept of temporal summation. However, this theory cannot explained the shifts in the psychometric slopes which will be studied in future work.

## 5.4 Limitations

In the method of constant stimuli, the repetition number of each amplitude ( $n$ ), step size to determine amplitude levels, the number of amplitude levels and total trials ( $N$ ) are important parameters to obtain accurate psychometric functions. In this study, the major limitation was the small repetition number for each amplitude. Since a higher number would not be feasible (due to motivation of subjects and the duration of the experiment), only 40 repetitions were used to estimate detection probabilities. Also six amplitude values were used because of similar time constraints. For the better fitting of data points, more amplitude levels should be tested.

In order to avoid subject bias, a two interval forced choice task was preferred. However, this task may have relatively larger estimation errors because the psychometric functions are compressed between 0.5 and 1 probability. This may also cause an asymmetry between the lower and upper asymptotes. In order to decrease errors trial numbers of each amplitude should be increased [77]. Particular to this thesis, we did not make sure that the stimulus was presented in equal numbers in the first and the second interval of the forced choice task. However, since the presentation trial was randomized with equal probability, we expect the effect of an imbalance to be small among all the trials (240 trials for each psychometric function).

Contactors size has an effect on both threshold and slope of the psychometric function for the Pacinian channel. As the contactor size increases, an increase in the slope and a decrease in the detection threshold are observed [75]. Since the middle finger tip has a small area, bigger contactor sizes could not be used in this experiment, which prevented some direct comparisons with previous studies. The vibrotactile sensitivity also changes with temperature [42]. In order to control skin surface temperature, a device which circulates the water in large contactors was used in previous studies. However, those contactors cannot be applied on the fingertip. Therefore the temperature only monitored in the current thesis. Since the measured temperatures were only between the 32 and 35 °C did not pose a problem for our study. The variation of skin surface temperature was low.

## 5.5 Future Work

As the next step, a population model may be created based on this experimental data. In other words, simulated spike responses from Pacinian fibers can be processed to incorporate the central mechanisms of temporal and spatial summation in the Pacinian channel. Previous models did not incorporate all the vibrotactile stimulus parameters such as amplitude, frequency, duration and contactor size. Therefore, the model can be useful to predict high frequency sensitivity of humans. This is particularly important for neuroprosthetic applications. Recently, there are significant efforts to incorporate the artificial touch to neuroprosthetic limbs. However, we still do not know how sensory afferent information is encoded in central neurons. The results of this thesis may be helpful to understand natural sensation and to develop algorithms for mimicking it in neuroprosthesis. Specifically, an artificially programmed temporal summation algorithm may modulate sensitivity to stimuli of different durations occurring in different environmental settings.

## REFERENCES

1. Berg, J., J. Dammann III, and F. Tenore, "Behavioral demonstration of a somatosensory neuroprosthesis," *IEEE Transactions on Neural Systems and Rehabilitation Engineering*, Vol. 21, no. 3, pp. 500–7, 2013.
2. Biddiss, E., D. Beaton, and T. Chau, "Consumer design priorities for upper limb prosthetics," *Disability and Rehabilitation: Assistive Technology*, Vol. 2, no. 6, pp. 346–57, 2007.
3. Dhillon, G., and K. Horch, "Direct neural sensory feedback and control of a prosthetic arm," *IEEE Transactions on Neural Systems and Rehabilitation Engineering*, Vol. 13, no. 4, pp. 468–72, 2005.
4. Green, B., "Vibrotactile temporal summation: Effect of frequency," *Sensory Processes*, Vol. 1, 1976.
5. Yıldız, M. Z., M. Özsaltık, and B. Güçlü, "Temporal summation is independent of frequency in the pacinian (p) tactile channel," in *Psychonomic Society, 52nd Annual Meeting, Seattle, WA*, p. 105, 2011.
6. Agache, P. G., C. Monneur, and J. L. Leveque, "Mechanical properties and young's modulus of human skin in vivo," *Arch Dermatol Res*, Vol. 269, no. 3, pp. 221–32, 1980.
7. Agache, P., and P. Humbert, *Measuring the skin*, Springer-Verlag, 2004.
8. Geerligs, M., "Skin layer mechanics," *TU Eindhoven*, 2010.
9. Sandby-Møller, J., and T. Poulsen, "Epidermal thickness at different body sites: relationship to age, gender, pigmentation, blood content, skin type and smoking habits," *Acta Dermato Venereologica*, Vol. 83, no. 6, pp. 410–13, 2003.
10. Hendriks, F., *Mechanical behaviour of human epidermal and dermal layers in vivo*. PhD thesis, Technische Universiteit Eindhoven, 2005.
11. Loewenstein, W., and R. Skalak, "Mechanical transmission in a pacinian corpuscle. an analysis and a theory," *The Journal of Physiology*, Vol. 182, no. 2, pp. 346–78, 1966.
12. Ilyinsky, O., "Processes of excitation and inhibition in single mechanoreceptors (pacinian corpuscles)," *Nature*, Vol. 208, no. 5008, pp. 351–53, 1965.
13. Kandel, E. and J. Schwartz, *Principles of Neural Science, Fifth Edition*, New York, NY, USA, McGraw-Hill Education, 2013.
14. Johansson, R., "Tactile sensibility in the human hand: receptive field characteristics of mechanoreceptive units in the glabrous skin area.," *The Journal of Physiology*, Vol. 281, no. 1, pp. 101–25, 1978.
15. Johnson, K., "The roles and functions of cutaneous mechanoreceptors," *Current Opinion in Neurobiology*, Vol. 11, no. 4, pp. 455–61, 2001.
16. Iggo, A., "Is the physiology of cutaneous receptors determined by morphology?," *Progress in Brain Research*, Vol. 43, pp. 15–31, 1976.

17. Vega-Bermudez, F., and K. Johnson, "Sa1 and ra receptive fields, response variability, and population responses mapped with a probe array," *Journal of Neurophysiology*, Vol. 81, no. 6, pp. 2701–10, 1999.
18. Johnson, K., and T. Yoshioka, "Tactile functions of mechanoreceptive afferents innervating the hand," *Journal of Clinical Neurophysiology*, Vol. 17, no. 6, pp. 539–58, 2000.
19. Guinard, D., Y. Usson, and C. Guillermet, "Ps-100 and nf 70-200 double immunolabeling for human digital skin meissner corpuscle 3d imaging," *Journal of Histochemistry & Cytochemistry*, Vol. 48, no. 2, pp. 295–302, 2000.
20. Bell, J., S. Bolanowski, and M. Holmes, "The structure and function of pacinian corpuscles: A review,"
21. Quindlen, J. and Stolarski, H., and M. Johnson, "A multiphysics model of the pacinian corpuscle," *Integrative Biology*, Vol. 8, no. 11, pp. 1111–25, 2016.
22. Purves, D., *Neuroscience Third Edition*, Sunderland, MA, USA, Sinauer Associates Inc, 2004.
23. Pease, D., and T. Quilliam, "Electron microscopy of the pacinian corpuscle," *The Journal of Cell Biology*, Vol. 3, no. 3, pp. 331–342, 1957.
24. Pawson, L., N. Slepecky, and S. Bolanowski, "Immunocytochemical identification of proteins within the pacinian corpuscle," *Somatosensory & Motor Research*, Vol. 17, no. 2, pp. 159–70, 2000.
25. Roberts, D., *Signals and Perception: The Fundamentals of Human Sensation*, Palgrave, 2002.
26. Verrillo, R., "Effect of contactor area on the vibrotactile threshold," *The Journal of the Acoustical Society of America*, Vol. 35, no. 12, pp. 1962–66, 1963.
27. Diamond, J., J. Gray, and D. Inman, "The relation between receptor potentials and the concentration of sodium ions," *The Journal of Physiology*, Vol. 142, no. 2, pp. 382–94, 1958.
28. Gray, J., and M. Sato, "Properties of the receptor potential in pacinian corpuscles," *The Journal of Physiology*, Vol. 122, no. 3, pp. 610–636, 1953.
29. Loewenstein, W., and R. Rathkamp, "Localization of generator structures of electric activity in a pacinian corpuscle," *Science*, Vol. 127, no. 3294, pp. 341–341, 1958.
30. Loewenstein, W., and R. Rathkamp, "The sites for mechano-electric conversion in a pacinian corpuscle," *The Journal of General Physiology*, Vol. 41, no. 6, pp. 1245–65, 1958.
31. Bolanowski, S. J., J. E. Schyuler, and N. B. Slepecky, "Semi-serial electron-micrographic reconstruction of putative transducer sites in pacinian corpuscles," *Somatosens Mot Res*, Vol. 2, no. 6, pp. 346–57, 2007.
32. Nishi, K., and M. Sato, "Depolarizing and hyperpolarizing receptor potentials in the non-myelinated nerve terminal in pacinian corpuscles," *The Journal of Physiology*, Vol. 199, no. 2, pp. 383–96, 1968.

33. Chambers, M., K. Andres, M. Duering, and A. Iggo, "The structure and function of the slowly adapting type ii mechanoreceptor in hairy skin," *Experimental Physiology*, Vol. 57, no. 4, pp. 417–45, 1972.
34. Gescheider, G.A., *Psychophysics: the fundamentals, Third Edition*, Mahwah, NJ, USA, Lawrence Erlbaum Associates, 1997.
35. Cauna, N., "Nerve supply and nerve endings in meissner's corpuscles," *Developmental Dynamics*, Vol. 99, no. 2, pp. 315–50, 1956.
36. Gray, J., and P. Matthews, "A comparison of the adaptation of the pacinian corpuscle with the accommodation of its own axon," *The Journal of Physiology*, Vol. 114, no. 4, pp. 454–64, 1951.
37. Iggo, A., and A. Muir, "The structure and function of a slowly adapting touch corpuscle in hairy skin," *The Journal of Physiology*, Vol. 200, no. 3, pp. 763–96, 1969.
38. Macefield, V., and C. Häger-Ross, "Control of grip force during restraint of an object held between finger and thumb: responses of cutaneous afferents from the digits," *Experimental Brain Research*, Vol. 108, no. 1, pp. 155–71, 1996.
39. Johansson, R., and G. Westling, "Roles of glabrous skin receptors and sensorimotor memory in automatic control of precision grip when lifting rougher or more slippery objects," *Experimental brain research*, Vol. 56, no. 3, pp. 550–64, 1984.
40. Brisben, A., S. Hsiao, and K. Johnson, "Detection of vibration transmitted through an object grasped in the hand," *Journal of Neurophysiology*, Vol. 81, no. 4, pp. 1548–58, 1999.
41. Freeman, A., and K. Johnson, "Cutaneous mechanoreceptors in macaque monkey: temporal discharge patterns evoked by vibration, and a receptor model," *The Journal of Physiology*, Vol. 323, no. 1, pp. 21–41, 1982.
42. Bolanowski, S. J., J. E. Schyuler, and N. B. Slepceky, "Temperature and criterion effects in a somatosensory subsystem: a neurophysiological and psychophysical study," *J Neurophysiol*, Vol. 48, no. 3, pp. 836–55, 1982.
43. Edin, B., "Quantitative analysis of static strain sensitivity in human mechanoreceptors from hairy skin," *The Journal of Physiology*, Vol. 67, no. 5, pp. 1105–13, 1992.
44. Olausson, H., J. Wessberg, and N. Kakuda, "Tactile directional sensibility: peripheral neural mechanisms in man," *Brain Research*, Vol. 866, no. 1, pp. 178–87, 2000.
45. Gardner, E., and B. Sklar, "Discrimination of the direction of motion on the human hand: a psychophysical study of stimulation parameters," *Journal of Neurophysiology*, Vol. 71, no. 6, pp. 2414–29, 1994.
46. Edin, B., and N. Johansson, "Skin strain patterns provide kinaesthetic information to the human central nervous system," *The Journal of Physiology*, Vol. 487, no. 1, pp. 243–51, 1995.
47. Collins, D., and A. Prochazka, "Movement illusions evoked by ensemble cutaneous input from the dorsum of the human hand," *The Journal of Physiology*, Vol. 496, no. 3, pp. 857–71, 1996.

48. Bolanowski, S. in *Fechner Day 98. Proceedings of the Fourteenth Annual Meeting of the International Society for Psychophysics*, pp. 103–108, 1998.
49. Talbot, W., I. Darian-Smith, and H. Kornhuber, “The sense of flutter-vibration: comparison of the human capacity with response patterns of mechanoreceptive afferents from the monkey hand,” *Journal of Neurophysiology*, Vol. 31, no. 2, pp. 301–34, 1968.
50. Gescheider, G., “Evidence in support of the duplex theory of mechanoreception,” *Sensory Processes*, 1976.
51. Capraro, A., R. Verrillo, and J. Zwislocki, “Psychophysical evidence for a triplex system of cutaneous mechanoreception,” *Sensory Processes*, Vol. 3, no. 4, pp. 334–52, 1979.
52. Craig, J., “Vibrotactile pattern recognition and masking,” *Active touch—the mechanism of recognition of objects by manipulation: A multi-disciplinary approach*, pp. 229–42, 1978.
53. Gescheider, G., B. Sklar, C. Van Doren, and R. Verrillo, “Vibrotactile forward masking: psychophysical evidence for a triplex theory of cutaneous mechanoreception,” *The Journal of the Acoustical Society of America*, Vol. 78, no. 2, pp. 534–43, 1985.
54. Bolanowski, J. S., and G. Gescheider, “Four channels mediate the mechanical aspects of touch,” *The Journal of the Acoustical Society of America*, Vol. 84, no. 5, pp. 1680–94, 1988.
55. Gescheider, G., *Psychophysics: Method and theory.*, Lawrence Erlbaum, 1976.
56. Gescheider, G., S. Bolanowski, K. Hall, K. Hoffman, and R. Verrillo, “The effects of aging on information-processing channels in the sense of touch: I. absolute sensitivity,” *Somatosensory & Motor Research*, Vol. 11, no. 4, pp. 345–57, 1994.
57. Gescheider, G., S. Bolanowski, and R. Verrillo, “Some characteristics of tactile channels,” *Behavioural Brain Research*, Vol. 148, no. 1, pp. 35–40, 2004.
58. Verrillo, R., and B. Jr.S.J., “The effects of skin temperature on the psychophysical responses to vibration on glabrous and hairy skin,” *The Journal of the Acoustical Society of America*, Vol. 80, no. 2, pp. 528–32, 1986.
59. Verrillo, R., “Temporal summation in vibrotactile sensitivity,” *The Journal of the Acoustical Society of America*, Vol. 37, no. 5, pp. 843–46, 1965.
60. Gescheider, G., S. Bolanowski, and J. Pope, “A four-channel analysis of the tactile sensitivity of the fingertip: frequency selectivity, spatial summation, and temporal summation,” *Somatosensory & Motor Research*, Vol. 19, no. 2, pp. 114–24, 2002.
61. Checkosky, C., and S. Bolanowski, “Effects of stimulus duration on the response properties of pacinian corpuscles: Implications for the neural code,” *The Journal of the Acoustical Society of America*, Vol. 91, no. 6, pp. 3372–80, 1992.
62. Frisina, R., and G. Gescheider, “Comparison of child and adult vibrotactile thresholds as a function of frequency and duration,” *Attention, Perception, & Psychophysics*, Vol. 22, no. 1, pp. 100–103, 1977.
63. Zwislocki, J., “Theory of temporal auditory summation,” *The Journal of the Acoustical Society of America*, Vol. 32, no. 8, pp. 1046–60, 1960.
64. Hartline, H. K., “Intensity and duration in the excitation of single photoreceptor units,” *Journal of Cellular Physiology*, Vol. 5, no. 2, pp. 229–47, 1934.

65. Zwislocki, J., "Temporal summation of loudness: An analysis," *The Journal of the Acoustical Society of America*, Vol. 46, no. 2B, pp. 431–41, 1969.
66. Algom, D., and H. Babkoff, "Auditory temporal integration at threshold: Theories and some implications of current research,"
67. Gescheider, G., K. Hoffman, and M. Harrison, "The effects of masking on vibrotactile temporal summation in the detection of sinusoidal and noise signals," *The Journal of the Acoustical Society of America*, Vol. 95, no. 2, pp. 1006–1016, 1994.
68. Johansson, R., U. Landstro, and R. Lundstro, "Responses of mechanoreceptive afferent units in the glabrous skin of the human hand to sinusoidal skin displacements," *Brain Research*, Vol. 244, no. 1, pp. 17–25, 1982.
69. Checkosky, C., and S. Bolanowski, "The effect of stimulus duration on frequency-response functions in the pacinian (p) channel," *Somatosensory & Motor research*, Vol. 11, no. 1, pp. 47–56, 1994.
70. Gescheider, G., M. Berryhill, R. Verrillo, and S. Bolanowski, "Vibrotactile temporal summation: probability summation or neural integration?," *Somatosensory & Motor Research*, Vol. 16, no. 3, pp. 229–42, 1999.
71. Güçlü, B., and Ç. Öztekin, "Tactile sensitivity of children: effects of frequency, masking, and the non-pacinian i psychophysical channel," *Journal of Experimental Child Psychology*, Vol. 98, no. 2, pp. 113–30, 2007.
72. Strasburger, H., "Converting between measures of slope of the psychometric function," *Attention, Perception, & Psychophysics*, Vol. 63, no. 8, pp. 1348–55, 2001.
73. Klein, S., "Measuring, estimating, and understanding the psychometric function: A commentary," *Attention, Perception, & Psychophysics*, Vol. 63, no. 8, pp. 1421–55, 2001.
74. Gescheider, G. A. and Capraro, A. J., R. D. Frisina, R. D. Hamer, and R. T. Verrillo, "The effects of a surround on vibrotactile thresholds.," *Sensory Processes*, Vol. 2, no. 2, pp. 99–115, 1978.
75. Gescheider, G. A., B. Güçlü, J. L. Sexton, S. Karalunas, and A. Fontana, "Spatial summation in the tactile sensory system: probability summation and neural integration," *Somatosens Mot Res*, Vol. 22, no. 4, pp. 255–68, 2005.
76. Güçlü, B., G. A. Gescheider, S. J. Bolanowski, and Y. İstefanopulos, "Population-response model for vibrotactile spatial summation," *Somatosens Mot Res*, Vol. 22, no. 4, pp. 239–53, 2005.
77. McKee, S. P., S. A. Klein, and D. Y. Teller, "Cstatistical properties of forced-choice psychometric functions: Implications of probit analysis," *Attention, Perception, & Psychophysics*, Vol. 37, no. 4, pp. 286–98, 1985.